PROCEEDINGS OF
THE ROYAL SOCIETY B
BIOLOGICAL SCIENCES

Head to Head: the case for fighting behaviour in *Megaloceros giganteus* using finite element analysis

Journal:	*Proceedings B*
Manuscript ID	RSPB-2019-1873.R1
Article Type:	Research
Date Submitted by the Author:	19-Sep-2019
Complete List of Authors:	Klinkhamer, Ada; University of New England, Environmental and Rural Sciences; Australian Age of Dinosaurs Museum of Natural History, Woodley, Nicholas; University of Newcastle Neenan, James; Oxford University Museum of Natural History Parr, William; University of New South Wales Clausen, Philip; University of Newcastle, School of Engineering Sanchez, Marcelo; University of Zürich, Palaeontologisches Institut und Museum Sansalone, Gabriele; University of New England Lister, Adrian; Natural History Museum, Palaeontology Wroe, Stephen; University of New England,
Subject:	Palaeontology < BIOLOGY, Behaviour < BIOLOGY, Biomechanics < BIOLOGY
Keywords:	Megaloceros, deer, finite element analysis, fighting
Proceedings B category:	Palaeobiology

Author-supplied statements

Relevant information will appear here if provided.

Ethics

Does your article include research that required ethical approval or permits?:
This article does not present research with ethical considerations

Statement (if applicable):
CUST_IF_YES_ETHICS :No data available.

Data

It is a condition of publication that data, code and materials supporting your paper are made publicly available. Does your paper present new data?:
Yes

Statement (if applicable):
Data is stored on UNEâ€™s data archive following University Policy, where it is registered in the Universityâ€™s metadata catalogue and in Research Data Australia.
https://rune.une.edu.au/web/handle/1959.11/27548
DOI: 10.25952/5d830b0e4a734.

Conflict of interest

I/We declare we have no competing interests

Statement (if applicable):
CUST_STATE_CONFLICT :No data available.

Authors' contributions

This paper has multiple authors and our individual contributions were as below

Statement (if applicable):
AJK wrote the first draft of the paper; SW, PC and MRSV conceived and designed the analysis; JMN and NW collected the data; NW, JMN, WP and GS performed the analysis; AML provided palaeobiological advice; AJK, NW and WP created tables and figures; all authors assisted in writing the final manuscript.

Head to Head: the case for fighting behaviour in *Megaloceros giganteus* using finite element analysis

Ada J. Klinkhamer [1] *, Nicholas Woodley [2], James M. Neenan [3], William C.H. Parr [4], Philip Clausen [2], Marcelo R. Sánchez-Villagra [5], Gabriele Sansalone [1], Adrian M. Lister [6] and Stephen Wroe [1]

[1] Function, Evolution and Anatomy Research lab, School of Environmental and Rural Science, University of New England, Armidale NSW 2351, Australia

[2] School of Engineering, University of Newcastle, Callaghan NSW 2308, Australia

[3] Oxford University Museum of Natural History, Parks Road, Oxford, OX1 3PW, United Kingdom

[4] Surgical and Orthopaedic Research Laboratories, School of Clinical Sciences, Faculty of Medicine, University of New South Wales, Randwick NSW 2031, Australia

[5] Paleontological Institute and Museum, University of Zurich, Karl Schmid Strasse 4, 8006 Zurich, Switzerland

[6] Department of Earth Sciences, Natural History Museum, London, SW7 5BD, United Kingdom

*ada.klinkhamer@gmail.com

Keywords: *Megaloceros*, deer, fighting, finite element analysis

Abstract

The largest antlers of any known deer species belonged to the extinct giant deer *Megaloceros giganteus*. It has been argued that their antlers were too large for use in fighting, instead being used only in ritualised displays to attract mates. Here we used finite element analysis (FEA) to test whether the antlers of *M. giganteus* could have withstood forces generated during fighting. We compared the mechanical performance of antlers in *M. giganteus* with three extant deer species: red deer (*Cervus elaphus*), fallow deer (*Dama dama*), and moose (*Alces alces*). Von Mises stress results suggest that *M. giganteus* was capable of withstanding some fighting loads, provided that their antlers interlocked proximally, and that it's antlers were best-adapted for withstanding loads from twisting rather than pushing actions, as are other deer with palmate antlers. We conclude that fighting in *M. giganteus* was likely more constrained and predictable than in extant deer.

Introduction

Understanding the evolution of exaggerated traits is one of the great challenges of evolutionary biology, particularly when dealing with extinct species in which the behaviour of organisms cannot be directly recorded (1). Among extinct mammals, few species can compete with the impressive structures of the middle to late Pleistocene giant deer, *Megaloceros giganteus* (Blumenbach, 1799) (2–4). With antlers reaching a span of 3.5 metres and weighing ~40kg (2,5,6), *M. giganteus* has been the subject of intense palaeobiological speculation, in particular on whether the function of these structures was purely for display or if they were also used for fighting. Here, to test whether they could have been used in fighting and better understand their biomechanics, we apply the computer-based method known as finite element analysis to the crania and antlers of *M. giganteus* and extant

47 deer species in a comparative context to investigate their mechanical performance and assess
48 their capacity to perform specific fighting behaviours.
49
50 Although some researchers have asserted that the antlers of *Megaloceros giganteus* could not
51 have resisted fighting loads because of their size (6–8), there can be little doubt that their
52 antlers played an important role in display behaviour. The antlers of *M. giganteus* were
53 oriented horizontally, compared to the more vertically oriented antlers of extant deer (Figure
54 1). When the animal stood facing an opponent the full breadth of the antlers were on show,
55 meaning it did not need to twist its head to display their size, allowing *M. giganteus* to
56 present an imposing image while also likely reducing twisting forces on the neck (5). The
57 position of the proximal brow tine differs from those in others such as *Cervus elaphus* by
58 pointing downwards. This has been interpreted as an appropriate orientation for protecting
59 the eye during fighting, but not for interlocking during a fight; however, there is little
60 evidence to support either assertion (2,4). Only a single study has attempted to predict actual
61 mechanical performance of *M. giganteus* antlers (9). Kitchener (9,10) tested a simple
62 biomechanical model of the antlers and analysed hydroxyapatite crystal structure using
63 neutron diffraction, finding that the preferred orientation of crystal structures strongly
64 supported the idea that its antlers could be used in fighting without risk of breakage.
65
66 In extant deer the use of antlers as weapons during fighting to determine dominance is well-
67 documented between males of relatively equal size (11–17). However, fighting risks serious
68 injury and antler breakage (12,15–20). Antler breakage can have a significant effect on future
69 fighting ability and may cause bodily injury, which has the potential to increase predation
70 risk (12,21). When fighting does occur, the mechanics can be described in two stages: an
71 initial clash and a pushing/twisting phase (12,15). The initial clash involves a collision

between the antlers of the two deer, requiring a capacity for the antler bone to resist impact loading. The pushing/twisting phase consists of a wrestling struggle with each of the deer using its antlers as levers to push and twist those of the opposing deer in order to knock the opponent off balance and injure it. In the case of *Megaloceros giganteus*, the pushing/twisting phase of the fight is of particular interest because the size and breadth of the antlers may have increased stresses during these activities.

In the present study we investigate the mechanical performance of antlers during pushing/twisting phases of a fight using a comparative finite element analysis approach (22–25) to answer the question: Did *Megaloceros giganteus* engage in pushing and twisting behaviours comparable to those of extant deer? We simulate and compare the mechanical performance of antlers in four different species: *Megaloceros giganteus*, *Cervus elaphus* (red deer), *Dama dama* (fallow deer), and *Alces alces* (elk), all of which belong to the Cervidae (26,27).

Materials

Extant deer species comprising a range of body masses and antler shapes were chosen for comparison with *Megaloceros giganteus*. *Dama dama* is thought to be the most closely related to *M. giganteus* on the basis of both morphological and DNA sequencing studies (27–29). *Alces alces* is the most similar to *M. giganteus* in body size, with comparable shoulder heights of approximately 1.8 metres (2). *Cervus elaphus* exhibits a differing antler morphology compared to the other taxa, with antlers that are multi-branched and unpalmated, as opposed to palmate. Specimen and scan information are given in Table 1.

Methods

Building models

Our modelling protocols largely followed previously published methods (23,25,30,31). For the extant taxa, Computed Tomography (CT) scan data were imported into Mimics (Materialise version 18.0) where the 'threshold' tool was used to generate individual 3D skull and antler models of each taxon which were then digitally 'stitched' together. The 3D models were exported to 3-Matic (Materialise version 10) where volume meshes preserving internal cavities were generated based on tet-4 elements. Material properties were derived from previous studies of *Cervus elaphus* antler bone that had an average Young's modulus of 7.1GPa and yield strength of 180MPa (41). The models were then imported into the finite element analysis package Strand7 for analysis (R3 version 15).

The modelling of antler geometry in all four deer in this analysis was based on cross-sectional data presented by Kitchener (9) who modelled cortical bone in *Megaloceros giganteus* and not cancellous bone. Observations of internal geometry of extant deer show that the densities of cancellous bone within the antlers of the same individual differ greatly. In addition, it is the cortical bone that bears most of the forces of fighting (32). For these reasons we follow Kitchener (9) and model only the cortical bone, treating the internal geometry as a hollow space. Models of all four species were done in the same way to allow for direct comparison. Generation of the *M. giganteus* skull model largely followed the above methodology for extant taxa; however, the antlers were too big to fit in a medical CT scanner. Therefore, the right *M. giganteus* antler was surface scanned and processed with Artec Studio 9 Education Software (Artec3D). As noted above, internal geometry for the antlers of *M. giganteus* was reconstructed following the internal geometry from Kitchener's (9) cross-sections as a guide (see Supplementary Figure S1 for detail on methodology). The right antler

reconstruction was mirrored to create a matching left antler (see Supplementary Figure S2). The antlers were positioned relative to the cranium and then attached in 3-Matic.

Our analyses were applied to both scaled and unscaled models. In scaled models, differences in size were removed by scaling all the models to the same surface area and applying the same uniform force to each model. In this analysis, comparisons are based on shape alone (33–35). We used the red deer (*Cervus elaphus*) as the reference model. We note that for this entirely comparative analysis the choice of reference model is arbitrary. The models were then scaled using the following relationship: $= \sqrt{\frac{SA}{SB}}$; where K is the scaling factor, SA is the surface area of the target model and SB is the surface area of the reference model.

Body mass and force estimates

For the unscaled comparison, we used estimates of body mass as proxies for the forces applied, as has been done in previous FEA-based studies (30,36,37). Our objective for this analysis was to determine performance in a wholly comparative context which incorporates allometry.

The average body mass of male *Cervus elaphus* ranges between 125kg and 185kg depending on the subspecies (38,39). *Dama dama* males have an average weight of 85-110kg (16,20), while male *Alces alces* have an average weight of about 485kg and a maximal weight of 730kg (38,40). Estimation of body mass for *Megaloceros* was based on recorded *Alces alces* body mass, as both have a similar shoulder height of around 1.8 meters and it has been argued that they were of comparable size (2). We have analysed two mass estimates in this study for all taxa; firstly a body mass representing the 'average', and then a 'maximal' mass to represent an 'extreme-case' (Table 2).

Force magnitudes were calculated using

$$F = m \times a$$

where m is the body mass of the animal (in kg), and a is the clash velocity divided by the deceleration time. Previously, Kitchener (9) determined a clash speed of 3 m/s and a deceleration time of 0.1s, producing an average deceleration of 30m/s^2. We therefore apply a = 30m/s^2 as a constant for all species in this analysis. Resulting forces were distributed evenly across contact points.

As an additional test, safety factors were calculated for all deer to compare stress responses to pushing and twisting actions. The 'safety factor' is the ratio between the strength of a structure and its maximum working stress; it is calculated by taking the yield stress of a material and dividing it by the maximum stress experienced by the object. In this case we applied yield stress as 180MPa based on previous work by Currey (41). However, our results are to be interpreted in an entirely comparative context and we do not present them as predictions of whether the antlers would break at specific loadings. Consequently the loadings at which antlers would 'fail', as well as safety factors are to be interpreted in relative terms only.

Modelling fighting posture

Our models were based on fighting behaviour of extant taxa for which fighting has been observed (11,12,14,16,17,20,42). All skulls were oriented in a 'fighting pose' in Strand7, i.e., as if the head was bent down so that the antlers face anteriorly (9,14). This fighting behaviour is observed in Old World deer like *Cervus elaphus* and *Dama dama,* and is also sometimes

observed in New World deer like *Alces alces* (10,43), however in order to provide a strictly comparative analysis we have standardised the fighting pose across all four taxa.

Forces were applied to each model at the point where the antlers were most likely to have contacted during pushing and twisting. For the deer with palmate antlers (*Megaloceros giganteus*, *Dama dama*, *Alces alces*) forces were applied to the more distal antlers as it has been observed that interlocking antlers on the more distal tines is common in deer with palmate antlers (14,16). For *Cervus elaphus* forces were applied closer to the base of the antlers. Placement of forces was estimated in *Megaloceros giganteus* based on a reconstruction of fighting conducted using 3D printed models. Supplementary Figure S3 details the placement of forces for each species. Restraints were placed at the back of the skull using rigid links. These links were attached via a single rigid link to a point in free space, which was restrained in translation and rotation.

Load cases

Loads were applied as either a unidirectional force to represent pushing, or as a torque to represent the twisting component of the fight. The 'pushing load' force was applied parallel to the neck restraint, while the 'twisting load' forces were applied as two forces of equal magnitudes but opposite directions which created torque and ensured no net lateral bending load was applied (Supplementary Figure S3). Pushing and twisting loads were analysed for all taxa at both average and maximum estimated body masses.

Two additional analyses ('alternative load') were conducted to test uncertainties in our methodology. Firstly, although we initially determined that forces in *Megaloceros giganteus* would have likely been placed on the more distal antlers, Kitchener (9,10,43) suggested

placement of forces at the antler's middle tine. We therefore test this alternative placement. A test was also conducted on the antlers of *Cervus elaphus*, where forces were placed more distally on the antlers, i.e., at the same point as those applied for our predicted loads in deer with palmate antlers. We did this to determine to what degree force placement could influence stress distribution.

A linear static solve was performed for each load case and results were displayed as contour plots showing von Mises stress with an upper limit of 180MPa, the approximate yield strength of antler bone (41). Stress distributions were then analysed and average peak stress was measured using the 'Peek' tool in Strand7. We reiterate that we do not presume here that our results indicate the actual loadings at which the antlers would have yielded. The upper limit applied here is only an arbitrary guide and our findings can only be considered in a wholly comparative context.

Results

Megaloceros giganteus

Scaled

Under a pushing load the *M. giganteus* model produced high stress in both the average (1480MPa) and maximum (2169MPa) load cases compared to the other three taxa analysed (Figure 2,3). Under a twisting load stress was slightly higher with peak stress for the average load case at 1723MPa, and 2541MPa under a maximum load (Figure 2,4). In the alternative *M. giganteus* model with a force placement at the middle tine there was a large overall reduction in stress magnitudes experienced through the antlers in both the average (351MPa) and maximum (512MPa) pushing loads (Figure 2,5). The alternative twisting load case showed an even greater decrease in stress in both average (147MPa) and maximum

(216MPa) models (Figure 2). The calculated safety factor for M. *giganteus* antlers was 0.7 (Supplementary Table 1).

Unscaled

Under a pushing load the *M. giganteus* model produced relatively high stress in both the average (195MPa) and maximum (295MPa) load cases (Figure 2,S4). Under a twisting load, peak stress was lower than in the pushing load with peak stress of 146MPa under an average load and 242MPa under a maximum load case (Figure 2,S5). The alternative *M. giganteus* model with a force placement at the middle tine had an overall reduction in stress magnitudes experienced through the antlers in both the average (89MPa) and maximum (134MPa) load cases under a pushing load (Figure 2,S6). The alternative twisting load also showed a decrease in stress in both average (114MPa) and maximum (180MPa) models (Figure S6).

Cervus elaphus

Scaled

A pushing load resulted in low stress in both the average (37MPa) and maximum (55MPa) models, i.e., less than in all other taxa (Figure 2,3). As with the pushing load, *C. elaphus* also experienced relatively low levels of stress in both average (41MPa) and maximum models (63MPa) under a twisting load (Figure 2,4). However, twisting produced higher peak stress levels than pushing. The alternative pushing load case, where force placement was located more distally on the antlers (Figure 2,5), showed an increase in peak stress levels compared to the original pushing load case in both the average (146MPa) and maximum (215MPa) models. Von Mises stress levels under the alternative twisting load case were also higher for both average (111MPa) and maximum (165MPa) load cases, yet here stress was lower than in the alternative pushing load case (Figure 2). The estimated safety factor for *C. elaphus* was 1.2 (Supplementary Table 1).

Unscaled

The pushing load resulted in low stress in both the average (37MPa) and maximum (55MPa) models, less than in all other taxa (Figure 2,S4). As with the pushing load, *C. elaphus* also experienced relatively low levels of stress in both average (41MPa) and maximum models (63MPa) under a twisting load (Figure 2,S5). However, twisting produced higher peak stress levels than pushing. The alternative pushing load case, where force placement was located more distally on the antlers (Figure 2,S6), showed an increase in peak stress levels compared to the original pushing load case in both the average (146MPa) and maximum (215MPa) models. Stress levels under the alternative twisting load case were also increased for both average (111MPa) and maximum (165MPa) load cases, yet here stress was lower than in the alternative pushing load case (Figure S6).

Dama dama

Scaled

Peak stress experienced under a pushing load in *D. dama* was higher under the maximal load (281MPa) than in the average load (190MPa) (Figure 2,3). Under a twisting load, peak stress was lower than in the pushing load, with the average load case resulting in stresses of 118MPa, and 174MPa for the maximum load (Figure 2,4). The highest stress was displayed on the antler beams, just above the brow tines. The calculated safety factor for *D. dama* was 1 (Supplementary Table 1).

Unscaled

Peak stress experienced under a pushing load in *D. dama* was high in the maximum load case (232MPa) but lower in the average load case (179MPa) (Figure 2,S4). Under a twisting load peak stress was reduced compared to a pushing load, with the average load case measuring stress at 92MPa, and 124MPa for the maximum load case (Figure 2,S5).

Alces alces

Scaled

Under a pushing load, peak stress in the average load case was 154MPa, and 224MPa under a maximum pushing load (Figure 2,3). Twisting showed a reduced level of stress compared to a pushing load in both average (64MPa) and maximum (96MPa) load cases (Figure 2,4). The estimated safety factor for *A. alces* was 1.7 (Supplementary Table 1).

Unscaled

Under a pushing load, stress magnitudes and patterns were similar to those found in the unscaled *Megaloceros giganteus* model (Figure 2,S4). Peak stress was 118MPa under an average load and 185MPa under maximum load. Twisting showed a reduced level of stress compared to a pushing load for both average (86MPa) and maximum (132MPa) loads (Figure 2,S5).

Discussion

With both the scaled and unscaled models, *Megaloceros giganteus* exhibited higher peak stresses than the three extant taxa in the main pushing and twisting load cases, indicating it was not well-adapted to performing this action. However, in the alternate model where forces were placed more proximally (at the middle tine) than the distal loading of the original load cases, results are much more in line with the extant taxa, particularly under a twisting action. Stresses were consistently higher in the scaled models compared to the unscaled models. This is particularly apparent in the scaled model of *M. giganteus.*

It has been previously proposed that deer with palmate antlers were more likely to interlock on the distal rather than the proximal tines compared to deer with other antler morphologies,

with palmation of the antler stiffening and strengthening the distal tines (14,16). However, in *Megaloceros giganteus* we saw much higher stress in our original model with forces placed distally compared with the alternative model with forces placed more proximally. This is likely because of the increased size of the antlers in this species, which increased their moment arm, therefore increasing stress and the risk of breakage (10). Similarly, when forces were placed more distally for the alternative *Cervus elaphus* model, there was also an increase in stress under both pushing and twisting loads compared to lower stress levels when forces were placed more proximally (original model). This suggests that *M. giganteus* was unlikely to also have interlocked its antlers distally during the pushing/twisting phase. In addition, although the results from *C. elaphus* match those of *M. giganteus*, the magnitude of stress is much lower, indicating that this taxon likely participated in more forceful fighting actions using the distal antlers compared to *M. giganteus*. This result further supports the proposition by Kitchener (10) that the antlers of *M. giganteus* were more likely to interlock at the mid-beam, where the middle tine is located.

The extant deer in this study with palmate antlers (*Dama dama*, *Alces alces*) showed lower levels of stress during twisting loads than in pushing loads. This is in contrast to *Cervus elaphus* which showed higher stress in twisting and lower stress in pushing. For *Megaloceros giganteus*, when forces were located distally, twisting stress was higher than pushing stress, but was lower with forces located more proximally. Since we have demonstrated above that it would have been more likely for *M. giganteus* to have interlocked their antlers more proximally, we believe this result adds quantitative support to previous observational studies suggesting that deer with palmate antlers are more likely to use a twisting movement to parry attacks from other deer, relative to deer with unpalmated antlers (14).

Finally, the calculation of safety factors can help determine the relative strength of *Megaloceros giganteus* compared with extant taxa. An object is at its most 'safe' when its safety factor is close to 1; too far below means a greater risk of failure while too far above indicates the object is over-engineered. In fighting terms, a low safety factor would more likely be observed if fighting were constrained and predictable, whereas a higher safety factor would be expected if applied forces were more variable (44). Overall, deer antlers generally have lower safety factors than the horns of other mammals because of their branched structure and annual regrowth; this is related to a low cost of failure (44). Calculated safety factors in this analysis were based on the scaled models. Results fall within a small range of 0.7 to 1.6. We excluded the original models of *Cervus elaphus* and *Megaloceros giganteus* in this calculation because of their excessively high and low results. *Megaloceros giganteus* has a lower safety factor (0.7) than any of the extant taxa, indicating a comparatively higher likelihood of fracture and suggesting that this taxon was participating in more predictable and ritualised fighting behaviours than other deer. Increasing the safety factor of *M. giganteus* antlers would require additional material to make them more resistant for variable fights. This would be particularly 'expensive' for *M. giganteus* as even small antlers are energetically costly to grow and regrow, and would also make the antlers too heavy to bear (9,15,32,44,45).

Conclusions

Overall, we interpret the evidence from our study as supportive of the proposition that *Megaloceros giganteus* was capable of withstanding some loads typically imposed in fighting behaviour among extant deer provided that their antlers interlocked proximally. However, high stresses in other simulations suggest that *M. giganteus* was less well-adapted to these behaviours than its extant counterparts. The low safety factor of *M. giganteus* antlers and the

high stress levels when loads were applied on the distal antlers indicates that its fighting behaviour was likely more constrained and predictable than that exhibited by some extant deer. More generally, we found that stress in all taxa was highest at the base of the antlers. In addition, all species in this analysis with palmate antlers exhibited lower levels of stress during twisting actions compared with pushing.

In this study we have not calculated the stresses produced during the initial impact action of fighting behaviour because the factors that influence the initial clash phase of a fight are dynamic and require multiple assumptions. Factors involved in the initial clash phase include: speed of collision, angle of clash, the effectiveness of bracing for collision, and the distribution of forces through the body. These could not be estimated with adequate accuracy. In addition, the restraints placed on the models in this analysis produced relatively rigid models which directed all forces through the antlers and skull. Our boundary conditions do not account for forces that would have been transferred to the neck and the rest of the body, or the action of the musculature in the neck and shoulders that would have acted to dampen the forces being applied. In research on bovids, it has been shown that most of the force from fighting is absorbed by the neck and body musculature rather than the horns (44). Neck musculature might have also played a role in providing additional force in fighting as has been suggested for the sabretooth cat (*Smilodon fatalis*) in delivering a canine bite (30).

By scaling the models to the same surface area, allometry is taken out of the equation and the influence of shape alone is compared. Here, by scaling the *Megaloceros giganteus* model to the much smaller surface area of *Cervus elaphus,* but applying the same loadings, very high stress results were returned in some load cases, and overall higher stress levels were observed in all models for *M. giganteus*. This suggests that if *M. giganteus* was the same size as *C.*

370 *elaphus,* its antlers would have been far more likely to break. However, our results for life-
371 sized, unscaled models suggest that, if the forces applied were directly proportional to body
372 mass, then the antlers of *M. giganteus* were far less likely to 'fail'. Thus, any capacity to
373 engage in fighting behaviour by *M. giganteus* was, at least in part, a consequence of its large
374 size. We further argue that, in reality, the forces applied by the two larger species (*Alces alces*
375 and *Megaloceros giganteus*) are likely to be over-estimates in relative terms. This is because
376 the forces that can be applied by any animal are proportional to cross-sectional areas and thus
377 to the squares of their linear dimensions. On the other hand their masses are proportional to
378 their volumes and hence to the cubes of their linear dimensions. Consequently, it has been
379 argued that maximum forces should be proportional to body mass$^{2/3}$ (46). If this holds true for
380 the taxa considered here, then both the actual loadings applied and von Mises stresses
381 returned for larger species in our unscaled models are relatively higher than might be
382 expected in real life. Thus, it may well be that our results for unscaled models overestimate
383 the stresses returned for *M. giganteus*, lending further support to our conclusion that the giant
384 deer was capable of fighting behaviours.
385

386 ## Acknowledgements

387 We thank Loïc Costeur and Bastien Mennecart from the Basel Natural History Museum and
388 Martina Schenkel from the Zoological Museum of the University of Zurich for access to
389 specimens, and the staff of the Basel University Hospital and Zurich University Hospital who
390 aided us with specimen scanning. We also thank the Australian Research Council for funding
391 this project through grants to SW (DP140102656 and DP140102659) and the Leverhume
392 Trust for funding an Early Career Research Fellowship to JMN (ECF-2017-360).
393

394 ## Data Accessibility

Data is stored on UNE's data archive following University Policy, where it is registered in the University's metadata catalogue and in Research Data Australia.

https://rune.une.edu.au/web/handle/1959.11/27548

DOI: 10.25952/5d830b0e4a734.

Author Contributions

AJK wrote the first draft of the paper; SW, PC and MRSV conceived and designed the analysis; JMN and NW collected the data; NW, JMN, WP and GS performed the analysis; AML provided palaeobiological advice; AJK, NW and WP created tables and figures; all authors assisted in writing the final manuscript.

Competing Interests

The authors declare no competing interests.

References

1. Padian K, Horner JR. The evolution of "bizarre structures" in dinosaurs: biomechanics, sexual selection, social selection or species recognition? Journal of Zoology. 2010;283(1):3–17.

2. Lister AM. The evolution of the giant deer, *Megaloceros giganteus* (Blumenbach). Zoological Journal of the Linnean Society. Wiley Online Library; 1994;112(1-2):65–100.

3. O'Driscoll Worman C, Kimbrell T. Getting to the hart of the matter: did antlers truly cause the extinction of the Irish elk? Oikos. Wiley Online Library; 2008;117(9):1397–405.

4. Vislobokova I. Giant deer: origin, evolution, role in the biosphere. Paleontological Journal. Springer; 2012;46(7):643–775.

5. Gould SJ. Positive allometry of antlers in the "Irish elk", Megaloceros giganteus. Nature. Nature Publishing Group; 1973;244(5415):375.

6. Gould SJ. The origin and function of "bizarre" structures: antler size and skull size in the "Irish Elk," *Megaloceros giganteus*. Evolution. Wiley Online Library;

1974;28(2):191–220.

7. Coope G. The ancient world of *Megaloceros*. Deer. 1973;2:974–7.

8. Geist V. The paradox of the great Irish stags. Natural History. 1986;95(3):54–65.

9. Kitchener A. Fighting behaviour of the extinct Irish elk. Modern Geology. 1987;11(1.28).

10. Kitchener A, Bacon G, Vincent J. Orientiation in Antler Bone and the Expected Stress Distribution, Studied by Neutron Diffraction. Biomimetics. 1994;2(4):297–307.

11. Barrette C. Fighting behavior of muntjac and the evolution of antlers. Evolution. Wiley Online Library; 1977;31(1):169–76.

12. Clutton-Brock TH, Albon S, Gibson R, Guinness FE. The logical stag: adaptive aspects of fighting in red deer (*Cervus elaphus* L.). Animal Behaviour. Elsevier; 1979;27:211–25.

13. Miura S. Social behavior and territoriality in male sika deer (*Cervus nippon* Temminck 1838) during the rut. Ethology. 1984;64(1):33–73.

14. Clutton-Brock T. The functions of antlers. Behaviour. Brill; 1982;79(2):108–24.

15. Lincoln G. Biology of antlers. Journal of Zoology. Wiley Online Library; 1992;226(3):517–28.

16. McElligott AG, Mattiangeli V, Mattiello S, Verga M, Reynolds CA, Hayden TJ. Fighting tactics of fallow bucks (*Dama dama*, Cervidae): reducing the risks of serious conflict. Ethology. 1998;104(9):789–803.

17. Bartos L, Fricová B, Bartosová-Vichová J, Panama J, Sustr P, Smidová E. Estimation of the probability of fighting in fallow deer (*Dama dama*) during the rut. Aggressive Behavior: Official Journal of the International Society for Research on Aggression. Wiley Online Library; 2007;33(1):7–13.

18. Clutton-Brock TH, Albon SD. The roaring of red deer and the evolution of honest advertisement. Behaviour. Brill; 1979;69(3):145–70.

19. Jennings DJ, Gammell MP, Carlin CM, Hayden TJ. Is the parallel walk between competing male fallow deer, *Dama dama*, a lateral display of individual quality? Animal behaviour. Elsevier; 2003;65(5):1005–12.

20. Jennings DJ, Gammell MP, Carlin CM, Hayden TJ. Effect of body weight, antler length, resource value and experience on fight duration and intensity in fallow deer. Animal Behaviour. 2004;68(1):213–21.

21. Jakobsson S, Brick O, Kullberg C. Escalated fighting behaviour incurs increased predation risk. Animal Behaviour. Academic Press; 1995;49(1):235–9.

22. Wroe S. Cranial mechanics compared in extinct marsupial and extant African lions using a finite-element approach. Journal of Zoology. 2008;274(4):332–9.

23. Attard MR, Parr WC, Wilson LA, Archer M, Hand SJ, Rogers TL, et al. Virtual Reconstruction and Prey Size Preference in the Mid Cenozoic Thylacinid, *Nimbacinus dicksoni* (Thylacinidae, Marsupialia). PloS One. Public Library of Science; 2014;9(4):e93088.

24. Button DJ, Barrett PM, Rayfield EJ. Comparative cranial myology and biomechanics of *Plateosaurus* and *Camarasaurus* and evolution of the sauropod feeding apparatus. Palaeontology. 2016;59(6):887–913.

25. Wroe S, Parr WC, Ledogar JA, Bourke J, Evans SP, Fiorenza L, et al. Computer simulations show that Neanderthal facial morphology represents adaptation to cold and high energy demands, but not heavy biting. Proceedings of the Royal Society B. 2018;285:20180085.

26. Blob RW, Snelgrove JM. Antler stiffness in moose (*Alces alces*): correlated evolution of bone function and material properties? J Morphol. 2006;267(9):1075–86.

27. Hughes S, Hayden TJ, Douady CJ, Tougard C, Germonpré M, Stuart A, et al. Molecular phylogeny of the extinct giant deer, *Megaloceros giganteus*. Molecular Phylogenetics and Evolution. 2006;40(1):285–91.

28. Lister A, Edwards CJ, Nock D, Bunce M, Van Pijlen I, Bradley D, et al. The phylogenetic position of the "giant deer" *Megaloceros giganteus*. Nature. 2005;438(7069):850.

29. Mennecart B, DeMiguel D, Bibi F, Rössner GE, Métais G, Neenan JM, et al. Bony labyrinth morphology clarifies the origin and evolution of deer. Scientific Reports. 2017;7(1):13176.

30. McHenry CR, Wroe S, Clausen PD, Moreno K, Cunningham E. Supermodeled sabercat, predatory behavior in Smilodon fatalis revealed by high-resolution 3D computer simulation. Proceedings of the National Academy of Sciences. 2007;104(41):16010–5.

31. Attard MR, Wilson LA, Worthy TH, Scofield P, Johnston P, Parr WC, et al. Moa diet fits the bill: virtual reconstruction incorporating mummified remains and prediction of biomechanical performance in avian giants. Proceedings of the Royal Society B. 2016;283:1–9.

32. Kitchener A. The evolution and mechanical design of horns and antlers. In: Rayner, JMV and Wootton RJ, editor. Biomechanics and Evolution. Cambridge University Press; 1991. p. 229–53.

33. Dumont E, Grosse I, Slater G. Requirements for comparing the performance of finite element models of biological structures. Journal of Theoretical Biology. 2009;256(1):96–103.

34. Piras P, Sansalone G, Teresi L, Moscato M, Profico A, Eng R, et al. Digging adaptation in insectivorous subterranean eutherians. The enigma of *Mesoscalops montanensis* unveiled by geometric morphometrics and finite element analysis. Journal of Morphology. 2015;276(10):1157–71.

35. Tsang L, Wilson L, Ledogar J, Wroe S, Attard M, Sansalone G. Raptor talon shape and biomechanical performance are controlled by relative prey size but not by allometry. Scientific Reports. 2019;9.

36. Ross CF. Finite element analysis in vertebrate biomechanics. The Anatomical Record. Wiley Online Library; 2005;283(2):253–8.

37. Bright JA. A review of paleontological finite element models and their validity. Journal of Paleontology. 2014;88(4):760–9.

38. Mitchell B, McCowan D, Nicholson I. Annual cycles of body weight and condition in Scottish red deer, *Cervus elaphus*. Journal of Zoology. 1976;180(1):107–27.

39. Janiszewski P, Kolasa S. Zoometric characteristics of red deer (*Cervus elaphus* L.) stags from Northern Poland. Baltic Forestry. 2006;12(1):122–7.

40. Aitken D, Child KN, Rea RV, Hjeljord OG. Age, sex, and seasonal differences of carcass weights of Moose from the Central Interior of British Columbia: a comparative analysis. Alces: A Journal Devoted to the Biology and Management of Moose. 2012;48:105–22.

41. Currey JD. Mechanical properties of bone tissues with greatly differing functions. Journal of Biomechanics. 1979;12(4):313–9.

42. Espmark Y. Rutting behaviour in reindeer (*Rangifer tarandus* L.). Animal Behaviour. Elsevier; 1964;12(1):159–63.

43. Kitchener A. The effect of behaviour and body weight on the mechanical design of horns. Journal of Zoology. 1985;205:191–203.

44. Kitchener A. An analysis of the forces of fighting of the blackbuck (*Antilope cervicapra*) and the bighorn sheep (*Ovis canadensis*) and the mechanical design of the horn of bovids. Journal of Zoology. 1988;214(1):1–20.

45. Goss RJ. Deer antlers: regeneration, function and evolution. Academic Press; 1983.

46. Alexander Rm. The maximum forces exerted by animals. Journal of Experimental Biology. 1985;115:231–8.

574 # Tables and Figures

575 Table 1: Specimens used in the analysis with specimen numbers and scan details. All skull
576 and antler material from each species came from individuals of comparable size. Institutional
577 abbreviations are as follows: NMB (Basel Natural History Museum), ZM (Zoological
578 Museum of the University of Zurich), USB (Basel University Hospital), USZ (Zurich
579 University Hospital).

Specimen name	Specimen number	CT Scans
Megaloceros giganteus	Skull: NMB G.2537	Siemens Sensation 16 at USB. 2030 slices; 0.75mm slice thickness
	Antler: ZM 20245	Artec Spider 3D surface scan with resolution of 0.5mm
Cervus elaphus	Skull: ZM 19206	Siemens Somatom Force at USZ. 1462 slices; 1.00mm slice thickness
	Antlers: ZM uncatalogued	Siemens Somatom Force at USZ. 5233 slices; 1.00mm slice thickness
Dama dama	Skull: NMB C1361	Siemens Sensation 16 at USB. 614 slices; 0.75m slice thickness
	Antlers: ZM 17911d	
Alces alces	Skull: NMB 10816	Siemens Sensation 16 at USB. 1013 slices; 0.75m slice thickness
	Antlers: ZM 17556	

580

581

582 Table 2: Body mass and force estimates for each deer species analysed in this study. Note
583 that weights and therefore forces for *Megaloceros giganteus* are based on *Alces alces*
584 estimates as has been outlined in 'Methods'.

Species	**Load case name**	**Mass (kg)**	**Force (N)**
Cervus elaphus	Average	126.2	3786
	Maximum	186.1	5583
Dama dama	Average	85	2550
	Maximum	110	3300
Alces alces	Average	484.4	14532
	Maximum	729.6	21888
Megaloceros giganteus	Average	484.4	14532
	Maximum	729.6	21888

585
586

Figure 1: 3D models of the four deer species analysed in this study. a) *Megaloceros giganteus*, b) *Cervus elaphus* (red deer), c) *Dama dama* (fallow deer), d) *Alces alces* (moose). Models have been displayed as approximately the same size for this figure.

Figure 2: Von Mises stress results in all four taxa under pushing and twisting loads for scaled and unscaled models. Table of results can be found in Supplementary Table 1.

Figure 3: Scaled finite element results of a pushing load. a) *Megaloceros giganteus* average load case, b) *Megaloceros giganteus* maximum load case, c) *Cervus elaphus* average load case, d) *Cervus elaphus* maximum load case, e) *Dama dama* average load case, f) *Dama dama* maximum load case, g) *Alces alces* average load case, h) *Alces alces* maximum load case.

Figure 4: Scaled finite element results of a twisting load. a) *Megaloceros giganteus* average load case, b) *Megaloceros giganteus* maximum load case, c) *Cervus elaphus* average load case, d) *Cervus elaphus* maximum load case, e) *Dama dama* average load case, f) *Dama dama* maximum load case, g) *Alces alces* average load case, h) *Alces alces* maximum load case.

Figure 5: Scaled finite element analysis results for alternative force placement on *Megaloceros* and *Cervus* under both pushing and twisting loads. Forces in *Megaloceros* were placed more narrowly than in the original analysis, while in *Cervus*, forces were placed more distally on the antlers. Pushing loads: a) *Megaloceros giganteus* average load case, b) *Megaloceros giganteus* maximum load case, c) *Cervus elaphus* average load case, d) *Cervus elaphus* maximum load case. Twisting loads: e) *Megaloceros giganteus* average load case, f) *Megaloceros giganteus* maximum load case, g) *Cervus elaphus* average load case, h) *Cervus elaphus* maximum load case.

Head to Head: the case for fighting behaviour in *Megaloceros giganteus* using finite element analysis

Ada J. Klinkhamer [1] *, Nicholas Woodley [2], James M. Neenan [3], William C.H. Parr [4], Philip Clausen [2], Marcelo R. Sánchez-Villagra [5], Gabriele Sansalone [1], Adrian M. Lister [6] and Stephen Wroe [1]

[1] Function, Evolution and Anatomy Research lab, School of Environmental and Rural Science, University of New England, Armidale NSW 2351, Australia

[2] School of Engineering, University of Newcastle, Callaghan NSW 2308, Australia

[3] Oxford University Museum of Natural History, Parks Road, Oxford, OX1 3PW, United Kingdom

[4] Surgical and Orthopaedic Research Laboratories, School of Clinical Sciences, Faculty of Medicine, University of New South Wales, Randwick NSW 2031, Australia

[5] Paleontological Institute and Museum, University of Zurich, Karl Schmid Strasse 4, 8006 Zurich, Switzerland

[6] Department of Earth Sciences, Natural History Museum, London, SW7 5BD, United Kingdom

*ada.klinkhamer@gmail.com

Keywords: *Megaloceros*, deer, fighting, finite element analysis

Abstract

The largest antlers of any known deer species belonged to the extinct giant deer *Megaloceros giganteus*. It has been argued that their antlers were too large for use in fighting, instead being used only in ritualised displays to attract mates. Here we used finite element analysis (FEA) to test whether the antlers of *M. giganteus* could have withstood forces generated during fighting ~~behaviour~~. We compared the mechanical performance of antlers in *M. giganteus* with three extant deer species: red deer (*Cervus elaphus*), fallow deer (*Dama dama*), and moose (*Alces alces*). Von Mises stress results suggest that *M. giganteus* was capable of withstanding some fighting loads, provided that their antlers interlocked proximally, and that it's antlers were ~~was~~ best-adapted for withstanding loads from twisting rather than pushing actions, as are other deer with palmate antlers. We conclude that fighting in *M. giganteus* was likely more constrained and predictable than in extant deer.

Introduction

Understanding the evolution of exaggerated traits is one of the great challenges of evolutionary biology, particularly when dealing with extinct species in which the behaviour of organisms cannot be directly recorded (1). Among extinct mammals, few species can compete with the impressive structures of the middle to late Pleistocene giant deer, *Megaloceros giganteus* (Blumenbach, 1799) (2–4). With antlers reaching a span of 3.5 metres and weighing ~40kg (2,5,6), *M. giganteus* has been the subject of intense palaeobiological speculation, in particular on whether the function of these structures was purely for display or if they were also used for fighting. Here, to test whether they could have been used in fighting and better understand their biomechanics, we apply the computer-based method known as finite element analysis to the crania and antlers of *M. giganteus* and extant

deer species in a comparative context to investigate their mechanical performance and assess their capacity to perform specific fighting behaviours.

Although some researchers have asserted that the antlers of *Megaloceros giganteus* could not have resisted fighting loads because of their size (6–8), there can be little doubt that their antlers played an important role in display behaviour. The antlers of *M. giganteus* were oriented horizontally, compared to the more vertically oriented antlers of extant deer (Figure 1). When the animal stood facing an opponent the full breadth of the antlers were on show, meaning it did not need to twist its head to display their size, allowing *M. giganteus* to present an imposing image while also likely reducing twisting forces on the neck (5). The position of the proximal browe~~ye~~ tine differs from those in others~~deer~~ such as *Cervus elaphus* by pointing downwards. This has been interpreted as an appropriate orientation for protecting the eye during fighting, but not for interlocking during a fight; however, there is little evidence to support either assertion (2,4). Only a single study has attempted to predict actual mechanical performance of *M. giganteus* antlers (9). Kitchener (9,10) tested a simple biomechanical model of the antlers and analysed hydroxyapatite crystal structure using neutron diffraction, finding that the preferred orientation of crystal structures strongly supported the idea that its antlers could be used in fighting without risk of breakage.

In extant deer the use of antlers as weapons during fighting to determine dominance is well-documented between males of relatively equal size (11–17). However, fighting risks serious injury and antler breakage (12,15–20). Antler breakage can have a significant effect on future fighting ability and may cause bodily injury, which has the potential to increase predation risk (12,21). When fighting does occur, the mechanics can be described in two stages: an initial clash and a pushing/twisting phase (12,15). The initial clash involves a collision

between the antlers of the two deer, requiring a capacity for the antler bone to resist impact loading. The pushing/twisting phase consists of a wrestling struggle with each of the deer using its antlers as levers to push and twist those of the opposing deer in order to knock the opponent off balance and injure it. In the case of *Megaloceros giganteus*, the pushing/twisting phase of the fight is of particular interest because the size and breadth of the antlers may have increased stresses during these activities.

In the present study we investigate the mechanical performance of antlers during pushing/twisting phases of a fight using a comparative finite element analysis approach (22–25) to answer the question: Did *Megaloceros giganteus* engage in pushing and twisting behaviours comparable to those of extant deer? We simulate and compare the mechanical performance of antlers in four different species: *Megaloceros giganteus*, *Cervus elaphus* (red deer), *Dama dama* (fallow deer), and *Alces alces* (elk), all of which belong to the Cervidae (26,27).

Materials

Extant deer species comprising a range of body masses and antler shapes were chosen for comparison with *Megaloceros giganteus*. *Dama dama* is thought to be the most closely related to *M. giganteus* on the basis of both morphological and DNA sequencing studies (27–29). *Alces alces* is the most similar to *M. giganteus* in body size, with comparable shoulder heights of approximately 1.8 metres (2). *Cervus elaphus* exhibits a differing antler morphology compared to the other taxa, with antlers that are multi-branched and unpalmated, as opposed to palmate. Specimen and scan information are given in Table 1.

Methods

Building models

Our modelling protocols largely followed previously published methods (23,25,30,31). For the extant taxa, Computed Tomography (CT) scan data were imported into Mimics (Materialise version 18.0) where the 'threshold' tool was used to generate individual 3D skull and antler models of each taxon which were then digitally 'stitched' together. The 3D models were exported to 3-Matic (Materialise version 10) where volume meshes ~~(~~preserving internal cavities~~)~~ ~~-~~were generated based on tet-4 elements. Material properties were derived from previous studies of *Cervus elaphus* antler bone that had~~-~~ an average Young's modulus of 7.1GPa and yield strength of 180MPa (41). The models were then~~before being~~ imported into the finite element analysis package Strand7 for analysis (R3 version 15)~~.~~.

The modelling of antler geometry in all four deer in this analysis was based on cross-sectional data presented by Kitchener (9) who modelled cortical bone in *Megaloceros giganteus* and not cancellous bone. Observations of internal geometry of extant deer show that the densities of cancellous bone within the antlers of the same individual differ greatly. In addition, it is the cortical bone that bears most of the forces of fighting (32). For these reasons we follow Kitchener (9) and model only the cortical bone, treating the internal geometry as a hollow space. Models of all four species were done in the same way to allow for direct comparison. Generation of the *M. giganteus* skull model largely followed the above methodology for extant taxa; however, the antlers were too big to fit in a medical CT scanner. Therefore, the right *M. giganteus* antler was surface scanned and processed with Artec Studio 9 Education Software (Artec3D). As noted above, internal geometry for the antlers of *M. giganteus* was reconstructed following the internal geometry from Kitchener's (9) cross-sections as a guide (see Supplementary Figure S1 for detail on methodology). The right antler

121 reconstruction was mirrored to create a matching left antler (see Supplementary Figure S2).
122 The antlers were positioned relative to the cranium and then attached in 3-Matic.
123
124 Our analyses were applied to both scaled and unscaled models. In scaled models, differences
125 in size were removed by scaling all the models to the same surface area and applying the
126 same uniform force to each model. In this analysis, comparisons are based on shape alone
127 (33–35). We used the red deer (*Cervus elaphus*) as the reference model. We note that for this
128 entirely comparative analysis the choice of reference model is arbitrary. The models were
129 then scaled using the following relationship: $= \sqrt{\frac{SA}{SB}}$; where K is the scaling factor, SA is the
130 surface area of the target model and SB is the surface area of the reference model.
131
132 **Body mass and force estimates**
133 For the unscaled comparison, we used estimates of body mass as proxies for the forces
134 applied, as has been done in previous FEA-based studies (30,36,37). Our objective for this
135 analysis was to determine performance in a wholly comparative context which incorporates
136 allometry.
137
138 The average body mass of male *Cervus elaphus* ranges between 125kg and 185kg depending
139 on the subspecies (38,39). *Dama dama* males have an average weight of 85-110kg (16,20),
140 while male *Alces alces* have an average weight of about 485kg and a maximal weight of
141 730kg (38,40). Estimation of body mass for *Megaloceros* was based on recorded *Alces alces*
142 body mass, as both have a similar shoulder height of around 1.8 meters and it has been
143 argued that they were of comparable size (2). We have analysed two mass estimates in this
144 study for all taxa; firstly a body mass representing the 'average', and then a 'maximal' mass
145 to represent an 'extreme-case' (Table 2).

Force magnitudes were calculated using

$$F = m \times a$$

where m is the body mass of the animal (in kg), and a is the clash velocity divided by the deceleration time. Previously, Kitchener (9) determined a clash speed of 3 m/s and a deceleration time of 0.1s, producing an average deceleration of 30m/s^2. We therefore apply a = 30m/s^2 as a constant for all species in this analysis. Resulting forces were distributed evenly across contact points.

As an additional test, safety factors were calculated for all deer to compare stress responses to pushing and twisting actions. The 'safety factor' is the ratio between the strength of a structure and its maximum working stress; it is calculated by taking the yield stress of a material and dividing it by the maximum stress experienced by the object. In this case we applied yield stress as 180MPa based on previous work by Currey (41). However, our results are to be interpreted in an entirely comparative context and we do not present them as predictions of whether the antlers would break at specific loadings. Consequently the loadings at which antlers would 'fail', as well as safety factors are to be interpreted in relative terms only.

Modelling fighting posture

Our models were based on fighting behaviour of extant taxa for which fighting has been observed (11,12,14,16,17,20,42). All skulls were oriented in a 'fighting pose' in Strand7, i.e., as if the head was bent down so that the antlers face anteriorly (9,14). This fighting behaviour is observed in Old World deer like *Cervus elaphus* and *Dama dama,* and is also sometimes

observed in New World deer like *Alces alces* (10,43), however in order to provide a strictly comparative analysis we have standardised the fighting pose across all four taxa.

Forces were applied to each model at the point where the antlers were most likely to have contacted during pushing and twisting. For the deer with palmate antlers (*Megaloceros giganteus*, *Dama dama*, *Alces alces*) forces were applied to the more distal antlers as it has been observed that interlocking antlers on the more distal tines is common in deer with palmate antlers (14,16). For *Cervus elaphus* forces were applied closer to the base of the antlers. Placement of forces was estimated in *Megaloceros giganteus* based on a reconstruction of fighting conducted using 3D printed models. Supplementary Figure S3 details the placement of forces for each species. Restraints were placed at the back of the skull using rigid links. These links were attached via a single rigid link to a point in free space, which was restrained in translation and rotation.

Load cases

Loads were applied as either a unidirectional force to represent pushing, or as a torque to represent the twisting component of the fight. The 'pushing load' force was applied parallel to the neck restraint, while the 'twisting load' forces were applied as two forces of equal magnitudes but opposite directions which created torque and ensured no net lateral bending load was applied (Supplementary ~~Information~~ Figure S3). Pushing and twisting loads were analysed for all taxa at both average and maximum estimated body masses.

Two additional analyses ('alternative load') were conducted to test uncertainties in our methodology. Firstly, although we initially determined that forces in *Megaloceros giganteus* would have likely been placed on the more distal antlers, Kitchener (9,10,43) suggested

placement of forces at the antler's middle tine. We therefore test this alternative placement. A test was also conducted on the antlers of *Cervus elaphus*, where forces were placed more distally on the antlers, i.e., at the same point as those applied for our predicted loads in deer with palmate antlers. We did this to determine to what degree force placement could influence stress distribution.

A linear static solve was performed for each load case and results were displayed as contour plots showing von Mises stress with an upper limit of 180MPa, the approximate yield strength of antler bone (41). Stress distributions were then analysed and average peak stress was measured using the 'Peek' tool in Strand7. We reiterate that we do not presume here that our results indicate the actual loadings at which the antlers would have yielded. The upper limit applied here is only an arbitrary guide and our findings can only be considered in a wholly comparative context.

Results

Megaloceros giganteus

Scaled

Under a pushing load the *M. giganteus* model produced high stress in both the average (1480MPa) and maximum (2169MPa) load cases compared to the other three taxa analysed (Figure 2,3~~; Table 3~~). Under a twisting load stress was slightly higher with peak stress for the average load case at 1723MPa, and 2541MPa under a maximum load (Figure 2,4~~3; Table 3~~). In the alternative *M. giganteus* model with a force placement at the middle tine there was a large overall reduction in stress magnitudes experienced through the antlers in both the average (351MPa) and maximum (512MPa) pushing loads (Figure 2,5~~4; Table 3~~). The alternative twisting load case showed an even greater decrease in stress in both average

(147MPa) and maximum (216MPa) models (Figure 2~~Table 3~~). The calculated safety factor for M. *giganteus* antlers was 0.7 (Supplementary Table 1).

Unscaled

Under a pushing load the *M. giganteus* model produced relatively high stress in both the average (195MPa) and maximum (295MPa) load cases (Figure 2~~5~~,~~;~~ S4~~Table 3~~). Under a twisting load, peak stress was lower than in the pushing load with peak stress of 146MPa under an average load and 242MPa under a maximum load case (Figure 2~~6~~;,~~-~~ S5~~Table 3~~). The alternative *M. giganteus* model with a force placement at the middle tine had an overall reduction in stress magnitudes experienced through the antlers in both the average (89MPa) and maximum (134MPa) load cases under a pushing load (Figure 2~~7~~,~~;~~ S6~~Table 3~~). The alternative twisting load ~~-~~also showed a decrease in stress in both average (114MPa) and maximum (180MPa) models (Figure S6~~Table 3~~).

Cervus elaphus

Scaled

A pushing load resulted in low stress in both the average (37MPa) and maximum (55MPa) models, i.e., less than in all other taxa (Figure 2,3~~; Table 3~~). As with the pushing load, *C. elaphus* also experienced relatively low levels of stress in both average (41MPa) and maximum models (63MPa) under a twisting load (Figure 2,4~~3; Table 3~~). However, twisting produced higher peak stress levels than pushing. The alternative pushing load case, where force placement was located more distally on the antlers (Figure 2,5~~4; Table 3~~), showed an increase in peak stress levels compared to the original pushing load case in both the average (146MPa) and maximum (215MPa) models. Von Mises stress levels under the alternative twisting load case were also higher for both average (111MPa) and maximum (165MPa) load

cases, yet here stress was lower than in the alternative pushing load case (Figure 2~~Table 3~~). The estimated safety factor for *C. elaphus* was 1.2 (Supplementary Table 1).

Unscaled

The pushing load resulted in low stress in both the average (37MPa) and maximum (55MPa) models, less than in all other taxa (Figure 2~~5~~,~~;~~ S4~~Table 3~~). As with the pushing load, *C. elaphus* also experienced relatively low levels of stress in both average (41MPa) and maximum models (63MPa) under a twisting load (Figure 2~~6~~,~~;~~ S5~~Table 3~~). However, twisting produced higher peak stress levels than pushing. The alternative pushing load case, where force placement was located more distally on the antlers (Figure 2,~~7;~~ S6 ~~Table 3~~), showed an increase in peak stress levels compared to the original pushing load case in both the average (146MPa) and maximum (215MPa) models. Stress levels under the alternative twisting load case were also increased for both average (111MPa) and maximum (165MPa) load cases, yet here stress was lower than in the alternative pushing load case (Figure~~Table~~ S6~~3~~).

Dama dama

Scaled

Peak stress experienced under a pushing load in *D. dama* was higher under the maximal load (281MPa) than in the average load (190MPa) (Figure 2,3~~; Table 3~~). Under a twisting load, peak stress was lower than in the pushing load, with the average load case resulting in stresses of 118MPa, and 174MPa for the maximum load (Figure 2,4~~3; Table 3~~). The highest stress was displayed on the antler beams, just above the brow tines. The calculated safety factor for *D. dama* was 1 (Supplementary Table 1).

Unscaled

Peak stress experienced under a pushing load in *D. dama* was high in the maximum load case (232MPa) but lower in the average load case (179MPa) (Figure 2,S4~~5; Table 3~~). Under a

twisting load peak stress was reduced compared to a pushing load, with the average load case measuring stress at 92MPa, and 124MPa for the maximum load case (Figure 2,S5~~6; Table 3~~).

Alces alces

Scaled

Under a pushing load, peak stress in the average load case was 154MPa, and 224MPa under a maximum pushing load (Figure 2,3~~; Table 3~~). Twisting showed a reduced level of stress compared to a pushing load in both average (64MPa) and maximum (96MPa) load cases (Figure 2,4~~3; Table 3~~). The estimated safety factor for *A. alces* was 1.7 (Supplementary Table 1).

Unscaled

Under a pushing load, stress magnitudes and patterns were similar to those found in the unscaled *Megaloceros giganteus* model (Figure 2,S4~~5; Table 3~~). Peak stress was 118MPa under an average load and 185MPa under maximum load. Twisting showed a reduced level of stress compared to a pushing load for both average (86MPa) and maximum (132MPa) loads (Figure 2,S5~~6; Table 3~~).

Discussion

With both the scaled and unscaled models, *Megaloceros giganteus* exhibited higher peak stresses than the three extant taxa in the main pushing and twisting load cases, indicating it was not well-adapted to performing this action. However, in the alternate model where forces were placed more proximally (at the middle tine) than the distal loading of the original load cases, results are much more in line with the extant taxa, particularly under a twisting action. Stresses were ~~was~~ consistently higher in the scaled models compared to the unscaled models. This is particularly apparent in the scaled model of *M. giganteus*.

294

295 It has been previously proposed that deer with palmate antlers were more likely to interlock
296 on the distal rather than the proximal tines compared to deer with other antler morphologies,
297 with palmation of the antler stiffening and strengthening the distal tines (14,16). However, in
298 *Megaloceros giganteus* we saw much higher stress in our original model with forces placed
299 distally compared with the alternative model with forces placed more proximally. This is
300 likely because of the increased size of the antlers in this species, which increased their ~~its~~
301 moment arm, therefore increasing stress and the risk of breakage (10). Similarly, when forces
302 were placed more distally for the alternative *Cervus elaphus* model, there was also an
303 increase in stress under both pushing and twisting loads compared to lower stress levels when
304 forces were placed more proximally (original model). This suggests that *M. giganteus* was
305 unlikely to also have interlocked its antlers distally during the pushing/twisting phase. In
306 addition, although the results from *C. elaphus* match those of *M. giganteus*, the magnitude of
307 stress is much lower, indicating that this taxon likely participated in more forceful fighting
308 actions using the distal antlers compared to *M. giganteus*. This result further supports the
309 proposition by Kitchener (10) that the antlers of *M. giganteus* were more likely to interlock at
310 the mid-beam, where the middle tine is located.

311

312 The extant deer in this study with palmate antlers (*Dama dama*, *Alces alces*) showed lower
313 levels of stress during twisting loads than in pushing loads. This is in contrast to *Cervus*
314 *elaphus* which showed higher stress in twisting and lower stress in pushing. For *Megaloceros*
315 *giganteus*, when forces were located distally, twisting stress was higher than pushing stress,
316 but was lower with forces located more proximally. Since we have demonstrated above that it
317 would have been more likely for *M. giganteus* to have interlocked their antlers more
318 proximally, we believe this result adds quantitative support to previous observational studies

suggesting that deer with palmate antlers are more likely to use a twisting movement to parry attacks from other deer, relative to deer with unpalmated antlers (14).

Finally, the calculation of safety factors can help determine the relative strength of *Megaloceros giganteus* compared with extant taxa. An object is at its most 'safe' when its safety factor is close to 1; too far below means a greater risk of failure while too far above indicates the object is over-engineered. In fighting terms, a low safety factor would more likely be observed if fighting were constrained and predictable, whereas a higher safety factor would be expected if applied forces were more variable (44). Overall, deer antlers generally have lower safety factors than the horns of other mammals because of their branched structure and annual regrowth; this is related to a low cost of failure (44). Calculated safety factors in this analysis were based on the scaled models. Results fall within a small range of 0.7 to 1.6. We excluded the original models of *Cervus elaphus* and *Megaloceros giganteus* in this calculation because of their excessively high and low results. *Megaloceros giganteus* has a lower safety factor (0.7) than any of the extant taxa, indicating a comparatively higher likelihood of fracture and suggesting that this taxon was participating in more predictable and ritualised fighting behaviours than other deer. Increasing the safety factor of *M. giganteus* antlers would require additional material to make them more resistant for variable fights. This would be particularly 'expensive' for *M. giganteus* as even small antlers are energetically costly to grow and regrow, and would also make the antlers too heavy to bear (9,15,32,44,45).

Conclusions

Overall, we interpret the evidence from our study as supportive of the proposition that *Megaloceros giganteus* was capable of withstanding some loads typically imposed in fighting

344 behaviour among extant deer provided that their antlers interlocked proximally. However,
345 high stresses in other simulations suggest that *M. giganteus* was less well-adapted to these
346 behaviours than its extant counterparts. The low safety factor of *M. giganteus* antlers and the
347 high stress levels when loads were applied on the distal antlers indicates that its fighting
348 behaviour was likely more constrained and predictable than that exhibited by some extant
349 deer. More generally, we found that stress in all taxa was highest at the base of the antlers. In
350 addition, all species in this analysis with palmate antlers exhibited lower levels of stress
351 during twisting actions compared with pushing.
352
353 In this study we have not calculated the stresses produced during the initial impact action of
354 fighting behaviour because the factors that influence the initial clash phase of a fight are
355 dynamic and require multiple assumptions. Factors involved in the initial clash phase include:
356 speed of collision, angle of clash, the effectiveness of bracing for collision, and the
357 distribution of forces through the body. These could not be estimated with adequate accuracy.
358 In addition, the restraints placed on the models in this analysis produced relatively rigid
359 models which directed all forces through the antlers and skull. Our boundary conditions do
360 not account for forces that would have been transferred to the neck and the rest of the body,
361 or the action of the musculature in the neck and shoulders that would have acted to dampen
362 the forces being applied. In research on bovids, it has been shown that most of the force from
363 fighting is absorbed by the neck and body musculature rather than the horns (44). Neck
364 musculature might have also played a role in providing additional force in fighting as has
365 been suggested for the sabretooth cat (*Smilodon fatalis*) in delivering a canine bite (30).
366
367 By scaling the models to the same surface area, allometry is taken out of the equation and the
368 influence of shape alone is compared. Here, by scaling the *Megaloceros giganteus* model to

the much smaller surface area of *Cervus elaphus,* but applying the same loadings, very high stress results were returned in some load cases, and overall higher stress levels were observed in all models for *M. giganteus*. This suggests that if *M. giganteus* was the same size as *C. elaphus,* its antlers would have been far more likely to break. However, our results for life-sized, unscaled models suggest that, if the forces applied were directly proportional to body mass, then the antlers of *M. giganteus* were far less likely to 'fail'. Thus, any capacity to engage in fighting behaviour by *M. giganteus* was, at least in part, a consequence of its large size. We further argue that, in reality, the forces applied by the two larger species (*Alces alces* and *Megaloceros giganteus*) are likely to be over-estimates in relative terms. This is because the forces that can be applied by any animal are proportional to cross-sectional areas and thus to the squares of their linear dimensions. On the other hand their masses are proportional to their volumes and hence to the cubes of their linear dimensions. Consequently, it has been argued that maximum forces should be proportional to body mass$^{2/3}$ (46). If this holds true for the taxa considered here, then both the actual loadings applied and von Mises stresses returned for larger species in our unscaled models are relatively higher than might be expected in real life. Thus, it may well be that our results for unscaled models overestimate the stresses returned for *M. giganteus*, lending further support to our conclusion that the giant deer was capable of fighting behaviours.

Acknowledgements

We thank Loïc Costeur and Bastien Mennecart from the Basel Natural History Museum and Martina Schenkel from the Zoological Museum of the University of Zurich for access to specimens, and the staff of the Basel University Hospital and Zurich University Hospital who aided us with specimen scanning. We also thank the Australian Research Council for funding

this project through grants to SW (DP140102656 and DP140102659) and the Leverhume Trust for funding an Early Career Research Fellowship to JMN (ECF-2017-360).

Author Contributions

AJK wrote the first draft of the paper; SW, PC and MRSV conceived and designed the analysis; JMN and NW collected the data; NW, JMN, WP and GS performed the analysis; AML provided palaeobiological advice; AJK, NW and WP created tables and figures; all authors assisted in writing the final manuscript.

Competing Interests

The authors declare no competing interests.

References

1. Padian K, Horner JR. The evolution of "bizarre structures" in dinosaurs: biomechanics, sexual selection, social selection or species recognition? Journal of Zoology. 2010;283(1):3–17.

2. Lister AM. The evolution of the giant deer, *Megaloceros giganteus* (Blumenbach). Zoological Journal of the Linnean Society. Wiley Online Library; 1994;112(1-2):65–100.

3. O'Driscoll Worman C, Kimbrell T. Getting to the hart of the matter: did antlers truly cause the extinction of the Irish elk? Oikos. Wiley Online Library; 2008;117(9):1397–405.

4. Vislobokova I. Giant deer: origin, evolution, role in the biosphere. Paleontological Journal. Springer; 2012;46(7):643–775.

5. Gould SJ. Positive allometry of antlers in the "Irish elk", Megaloceros giganteus. Nature. Nature Publishing Group; 1973;244(5415):375.

6. Gould SJ. The origin and function of "bizarre" structures: antler size and skull size in the "Irish Elk," *Megaloceros giganteus*. Evolution. Wiley Online Library; 1974;28(2):191–220.

7. Coope G. The ancient world of *Megaloceros*. Deer. 1973;2:974–7.

8. Geist V. The paradox of the great Irish stags. Natural History. 1986;95(3):54–65.

9. Kitchener A. Fighting behaviour of the extinct Irish elk. Modern Geology. 1987;11(1.28).

10. Kitchener A, Bacon G, Vincent J. Orientiation in Antler Bone and the Expected Stress Distribution, Studied by Neutron Diffraction. Biomimetics. 1994;2(4):297–307.

11. Barrette C. Fighting behavior of muntjac and the evolution of antlers. Evolution. Wiley Online Library; 1977;31(1):169–76.

12. Clutton-Brock TH, Albon S, Gibson R, Guinness FE. The logical stag: adaptive aspects of fighting in red deer (*Cervus elaphus* L.). Animal Behaviour. Elsevier; 1979;27:211–25.

13. Miura S. Social behavior and territoriality in male sika deer (*Cervus nippon* Temminck 1838) during the rut. Ethology. 1984;64(1):33–73.

14. Clutton-Brock T. The functions of antlers. Behaviour. Brill; 1982;79(2):108–24.

15. Lincoln G. Biology of antlers. Journal of Zoology. Wiley Online Library; 1992;226(3):517–28.

16. McElligott AG, Mattiangeli V, Mattiello S, Verga M, Reynolds CA, Hayden TJ. Fighting tactics of fallow bucks (*Dama dama*, Cervidae): reducing the risks of serious conflict. Ethology. 1998;104(9):789–803.

17. Bartos L, Fricová B, Bartosová-Vichová J, Panama J, Sustr P, Smidová E. Estimation of the probability of fighting in fallow deer (*Dama dama*) during the rut. Aggressive Behavior: Official Journal of the International Society for Research on Aggression. Wiley Online Library; 2007;33(1):7–13.

18. Clutton-Brock TH, Albon SD. The roaring of red deer and the evolution of honest advertisement. Behaviour. Brill; 1979;69(3):145–70.

19. Jennings DJ, Gammell MP, Carlin CM, Hayden TJ. Is the parallel walk between competing male fallow deer, *Dama dama*, a lateral display of individual quality? Animal behaviour. Elsevier; 2003;65(5):1005–12.

20. Jennings DJ, Gammell MP, Carlin CM, Hayden TJ. Effect of body weight, antler length, resource value and experience on fight duration and intensity in fallow deer. Animal Behaviour. 2004;68(1):213–21.

21. Jakobsson S, Brick O, Kullberg C. Escalated fighting behaviour incurs increased predation risk. Animal Behaviour. Academic Press; 1995;49(1):235–9.

22. Wroe S. Cranial mechanics compared in extinct marsupial and extant African lions using a finite-element approach. Journal of Zoology. 2008;274(4):332–9.

23. Attard MR, Parr WC, Wilson LA, Archer M, Hand SJ, Rogers TL, et al. Virtual Reconstruction and Prey Size Preference in the Mid Cenozoic Thylacinid, *Nimbacinus dicksoni* (Thylacinidae, Marsupialia). PloS One. Public Library of Science; 2014;9(4):e93088.

24. Button DJ, Barrett PM, Rayfield EJ. Comparative cranial myology and biomechanics of *Plateosaurus* and *Camarasaurus* and evolution of the sauropod feeding apparatus. Palaeontology. 2016;59(6):887–913.

25. Wroe S, Parr WC, Ledogar JA, Bourke J, Evans SP, Fiorenza L, et al. Computer simulations show that Neanderthal facial morphology represents adaptation to cold and high energy demands, but not heavy biting. Proceedings of the Royal Society B. 2018;285:20180085.

26. Blob RW, Snelgrove JM. Antler stiffness in moose (*Alces alces*): correlated evolution of bone function and material properties? J Morphol. 2006;267(9):1075–86.

27. Hughes S, Hayden TJ, Douady CJ, Tougard C, Germonpré M, Stuart A, et al. Molecular phylogeny of the extinct giant deer, *Megaloceros giganteus*. Molecular Phylogenetics and Evolution. 2006;40(1):285–91.

28. Lister A, Edwards CJ, Nock D, Bunce M, Van Pijlen I, Bradley D, et al. The phylogenetic position of the "giant deer" *Megaloceros giganteus*. Nature. 2005;438(7069):850.

29. Mennecart B, DeMiguel D, Bibi F, Rössner GE, Métais G, Neenan JM, et al. Bony labyrinth morphology clarifies the origin and evolution of deer. Scientific Reports. 2017;7(1):13176.

30. McHenry CR, Wroe S, Clausen PD, Moreno K, Cunningham E. Supermodeled sabercat, predatory behavior in Smilodon fatalis revealed by high-resolution 3D computer simulation. Proceedings of the National Academy of Sciences. 2007;104(41):16010–5.

31. Attard MR, Wilson LA, Worthy TH, Scofield P, Johnston P, Parr WC, et al. Moa diet fits the bill: virtual reconstruction incorporating mummified remains and prediction of biomechanical performance in avian giants. Proceedings of the Royal Society B. 2016;283:1–9.

32. Kitchener A. The evolution and mechanical design of horns and antlers. In: Rayner, JMV and Wootton RJ, editor. Biomechanics and Evolution. Cambridge University Press; 1991. p. 229–53.

33. Dumont E, Grosse I, Slater G. Requirements for comparing the performance of finite element models of biological structures. Journal of Theoretical Biology. 2009;256(1):96–103.

34. Piras P, Sansalone G, Teresi L, Moscato M, Profico A, Eng R, et al. Digging adaptation in insectivorous subterranean eutherians. The enigma of *Mesoscalops montanensis* unveiled by geometric morphometrics and finite element analysis. Journal of Morphology. 2015;276(10):1157–71.

35. Tsang L, Wilson L, Ledogar J, Wroe S, Attard M, Sansalone G. Raptor talon shape and biomechanical performance are controlled by relative prey size but not by allometry. Scientific Reports. 2019;9.

36. Ross CF. Finite element analysis in vertebrate biomechanics. The Anatomical Record. Wiley Online Library; 2005;283(2):253–8.

37. Bright JA. A review of paleontological finite element models and their validity. Journal of Paleontology. 2014;88(4):760–9.

38. Mitchell B, McCowan D, Nicholson I. Annual cycles of body weight and condition in Scottish red deer, *Cervus elaphus*. Journal of Zoology. 1976;180(1):107–27.

39. Janiszewski P, Kolasa S. Zoometric characteristics of red deer (*Cervus elaphus* L.) stags from Northern Poland. Baltic Forestry. 2006;12(1):122–7.

40. Aitken D, Child KN, Rea RV, Hjeljord OG. Age, sex, and seasonal differences of carcass weights of Moose from the Central Interior of British Columbia: a comparative analysis. Alces: A Journal Devoted to the Biology and Management of Moose. 2012;48:105–22.

41. Currey JD. Mechanical properties of bone tissues with greatly differing functions. Journal of Biomechanics. 1979;12(4):313–9.

42. Espmark Y. Rutting behaviour in reindeer (*Rangifer tarandus* L.). Animal Behaviour. Elsevier; 1964;12(1):159–63.

43. Kitchener A. The effect of behaviour and body weight on the mechanical design of horns. Journal of Zoology. 1985;205:191–203.

44. Kitchener A. An analysis of the forces of fighting of the blackbuck (*Antilope cervicapra*) and the bighorn sheep (*Ovis canadensis*) and the mechanical design of the horn of bovids. Journal of Zoology. 1988;214(1):1–20.

45. Goss RJ. Deer antlers: regeneration, function and evolution. Academic Press; 1983.

46. Alexander Rm. The maximum forces exerted by animals. Journal of Experimental Biology. 1985;115:231–8.

570 # Tables and Figures

571 Table 1: Specimens used in the analysis with specimen numbers and scan details. All skull
572 and antler material from each species came from individuals of comparable size. Institutional
573 abbreviations are as follows: NMB (Basel Natural History Museum), ZM (Zoological
574 Museum of the University of Zurich), USB (Basel University Hospital), USZ (Zurich
575 University Hospital).

Specimen name	Specimen number	CT Scans
Megaloceros giganteus	Skull: NMB G.2537	Siemens Sensation 16 at USB. 2030 slices; 0.75mm slice thickness
	Antler: ZM 20245	Artec Spider 3D surface scan with resolution of 0.5mm
Cervus elaphus	Skull: ZM 19206	Siemens Somatom Force at USZ. 1462 slices; 1.00mm slice thickness
	Antlers: ZM uncatalogued	Siemens Somatom Force at USZ. 5233 slices; 1.00mm slice thickness
Dama dama	Skull: NMB C1361	Siemens Sensation 16 at USB. 614 slices; 0.75m slice thickness
	Antlers: ZM 17911d	
Alces alces	Skull: NMB 10816	Siemens Sensation 16 at USB. 1013 slices; 0.75m slice thickness
	Antlers: ZM 17556	

576

577

578 Table 2: Body mass and force estimates for each deer species analysed in this study. Note
579 that weights and therefore forces for *Megaloceros giganteus* are based on *Alces alces*
580 estimates as has been outlined in 'Methods'.

Species	**Load case name**	**Mass (kg)**	**Force (N)**
Cervus elaphus	Average	126.2	3786
	Maximum	186.1	5583
Dama dama	Average	85	2550
	Maximum	110	3300
Alces alces	Average	484.4	14532
	Maximum	729.6	21888
Megaloceros giganteus	Average	484.4	14532
	Maximum	729.6	21888

581
582

583 Table 3: Peak stress results for scaled and unscaled models according to load case in all four
584 species analysed. Safety factor calculations based on scaled model results.

Species	Load case		Scaled peak stress (MPa)	Unscaled peak stress (MPa)	Safety Factor
Megaloceros giganteus	Pushing	Average	1480	195	0.1
		Maximum	2169	295	0.1
		Average (alternative)	351	89	0.5
		Maximum (alternative)	512	134	0.4
	Twisting	Average	1723	146	0.1
		Maximum	2541	242	0.1
		Average (alternative)	147	114	1.2
		Maximum (alternative)	216	180	0.8
Cervus elaphus	Pushing	Average	37	37	4.9
		Maximum	55	55	3.3
		Average (alternative)	146	146	1.2
		Maximum (alternative)	215	215	0.8
	Twisting	Average	41	41	4.4
		Maximum	63	63	2.9
		Average (alternative)	111	111	1.6
		Maximum (alternative)	165	165	1.1
Dama dama	Pushing	Average	190	179	0.9
		Maximum	281	232	0.6
	Twisting	Average	118	92	1.5
		Maximum	174	124	1.0
Alces alces	Pushing	Average	154	118	1.2
		Maximum	224	185	0.8
	Twisting	Average	64	86	2.8
		Maximum	96	132	1.9

585

586

587

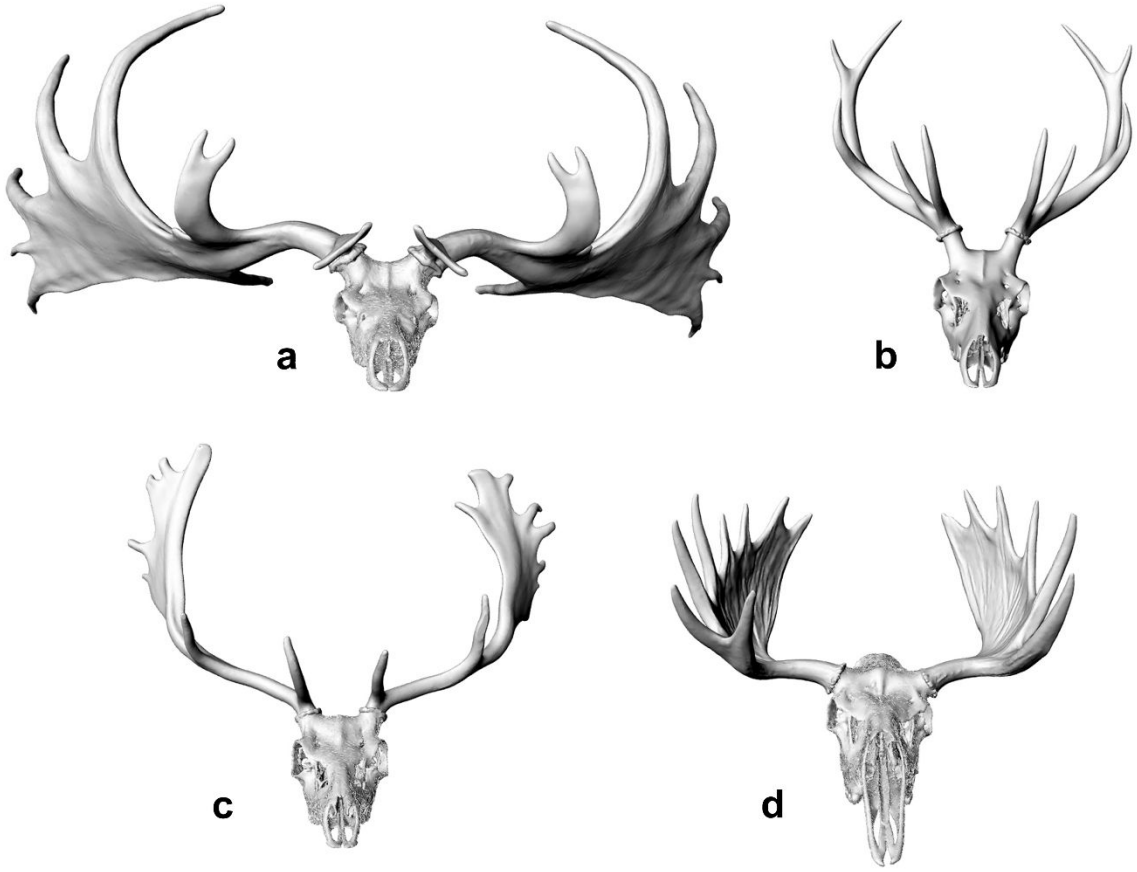

588

589 Figure 1: 3D models of the four deer species analysed in this study. a) *Megaloceros*
590 *giganteus*, b) *Cervus elaphus* (red deer), c) *Dama dama* (fallow deer), d) *Alces alces* (moose).
591 Models have been scaled to approximate same size for this figure.

592

Figure 2: Von Mises stress results in all four taxa under pushing and twisting loads for scaled and unscaled models. Table of results can be found in Supplementary Table 1.

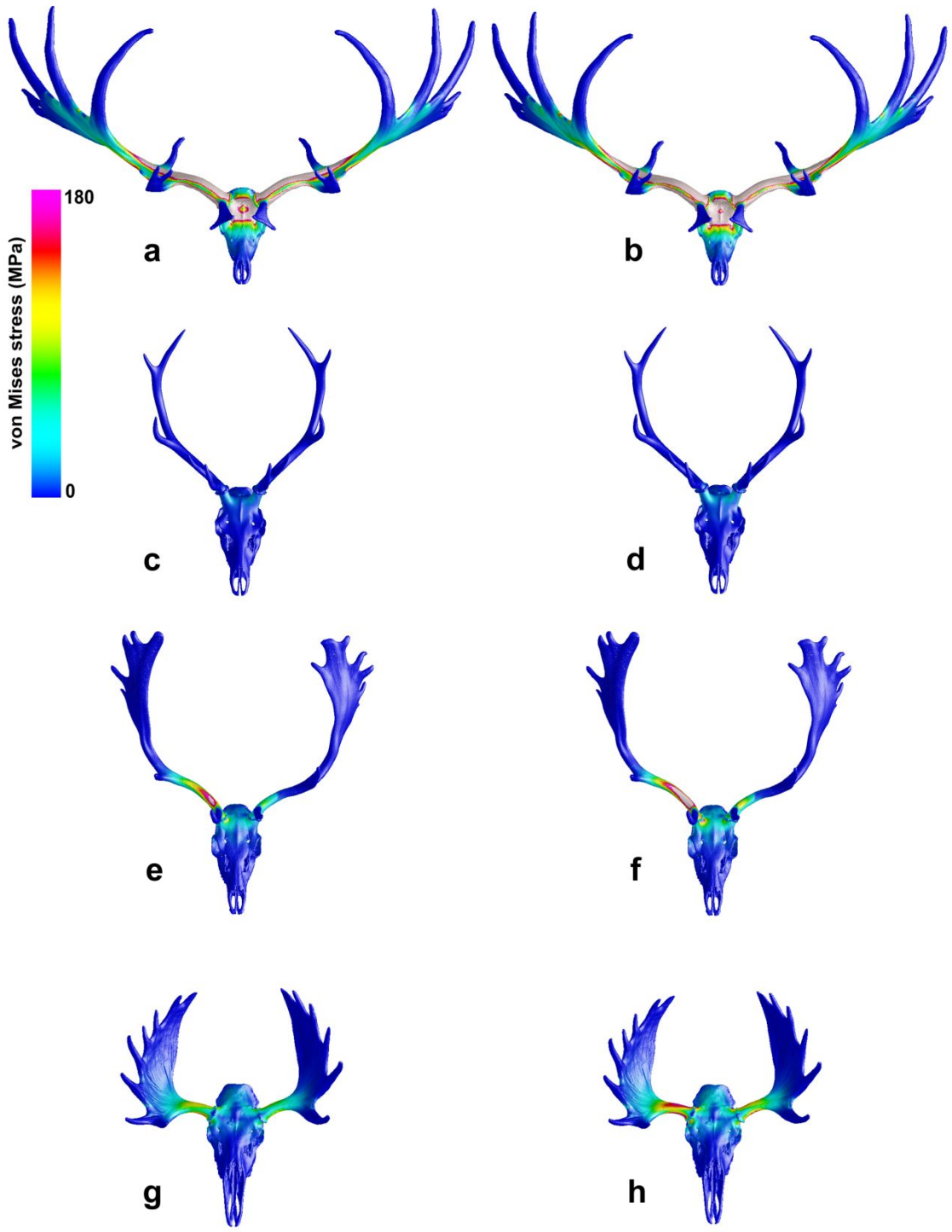

Figure 3~~2~~: Scaled finite element results of a pushing load. a) *Megaloceros giganteus* average load case, b) *Megaloceros giganteus* maximum load case, c) *Cervus elaphus* average load case, d) *Cervus elaphus* maximum load case, e) Fallow Deer average load case, f) Fallow Deer maximum load case, g) Moose average load case, h) Moose maximum load case.

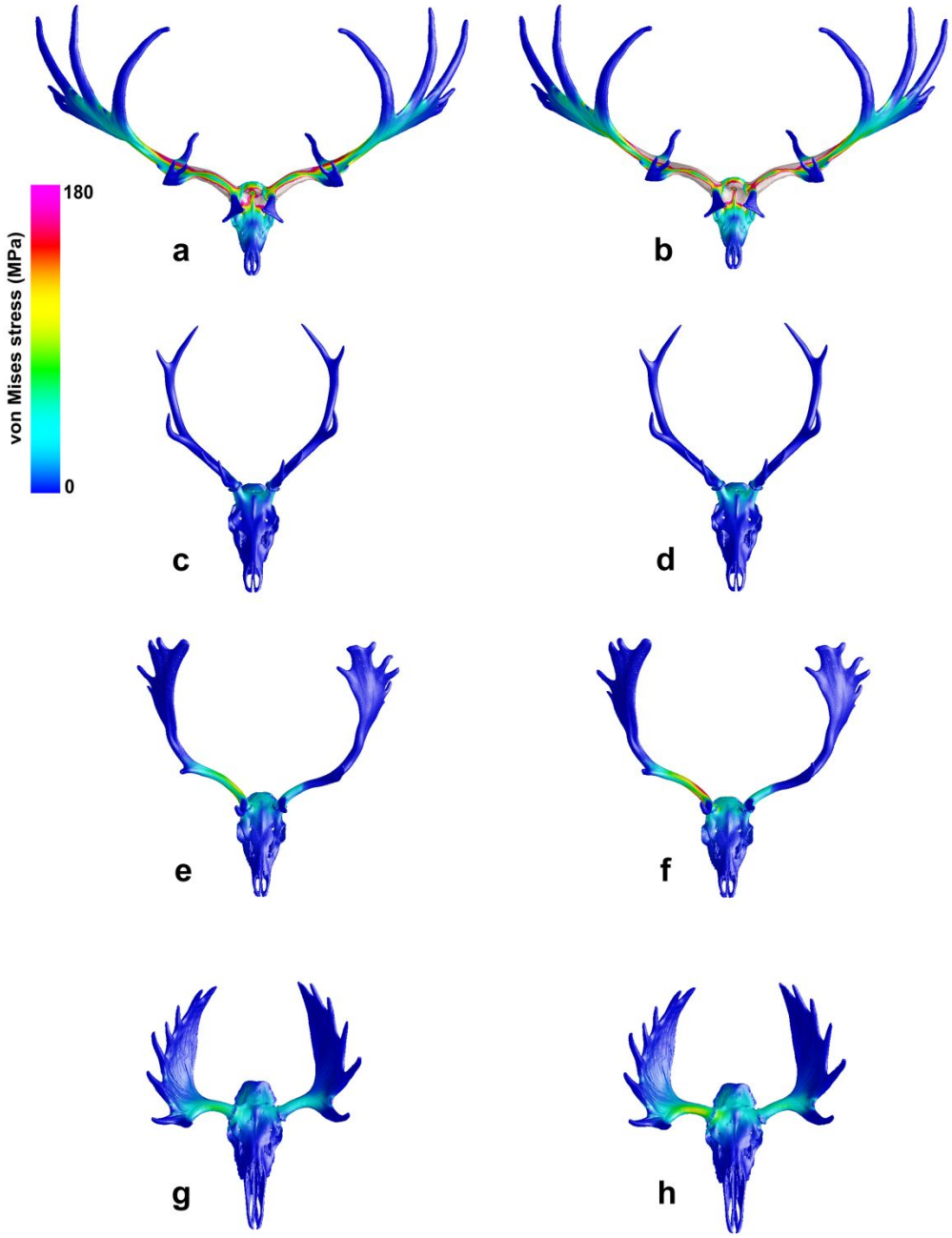

Figure 4~~3~~: Scaled finite element results of a twisting load. a) *Megaloceros giganteus* average load case, b) *Megaloceros giganteus* maximum load case, c) *Cervus elaphus* average load case, d) *Cervus elaphus* maximum load case, e) Fallow Deer average load case, f) Fallow Deer maximum load case, g) Moose average load case, h) Moose maximum load case.

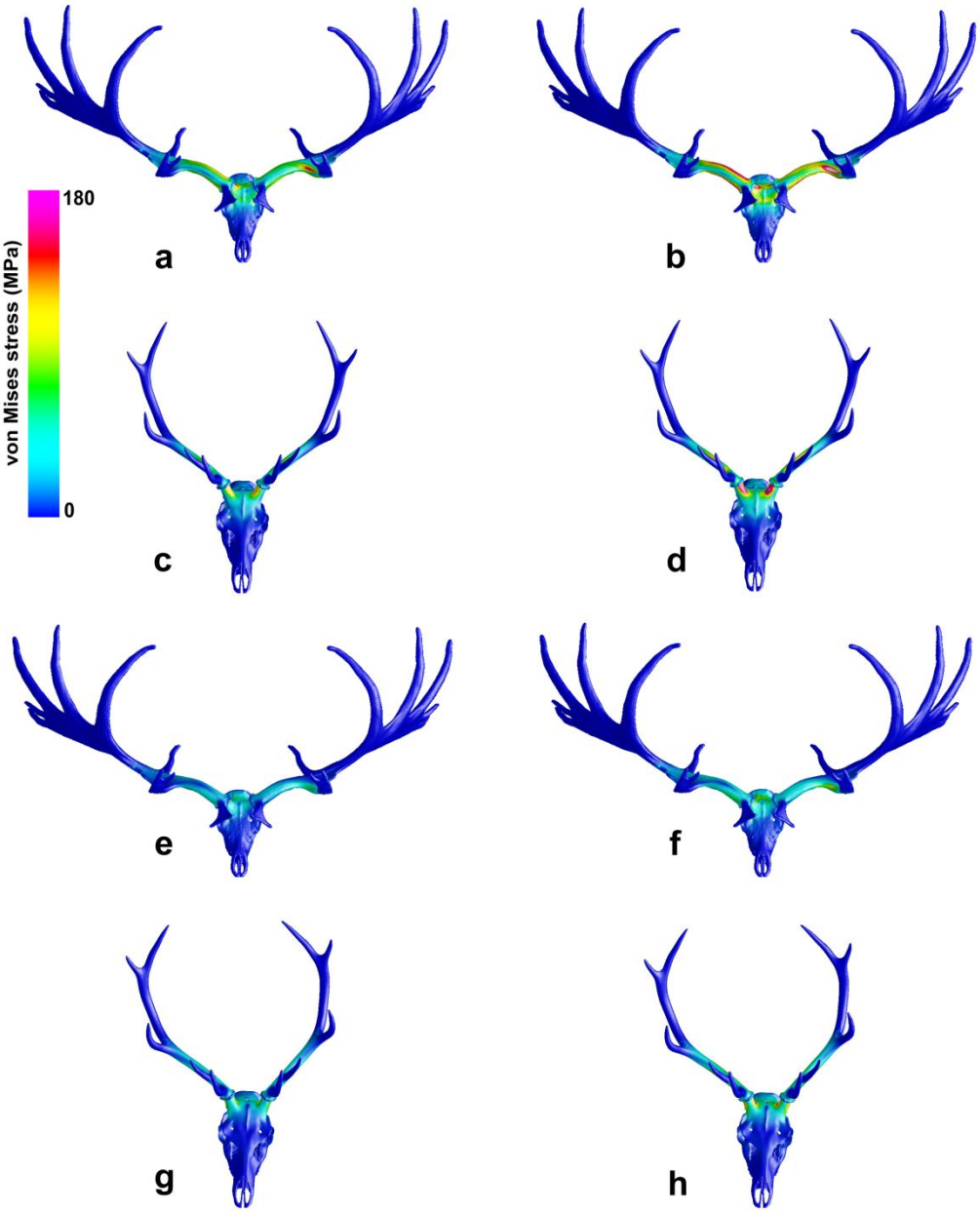

Figure 54: Scaled finite element analysis results for alternative force placement on *Megaloceros* and *Cervus* under both pushing and twisting loads. Forces in *Megaloceros* were placed more narrowly than in the original analysis, while in *Cervus*, forces were placed more distally on the antlers. Pushing loads: a) *Megaloceros giganteus* average load case, b) *Megaloceros giganteus* maximum load case, c) *Cervus elaphus* average load case, d) *Cervus elaphus* maximum load case. Twisting loads: e) *Megaloceros giganteus* average load case, f) *Megaloceros giganteus* maximum load case, g) *Cervus elaphus* average load case, h) *Cervus elaphus* maximum load case.

617

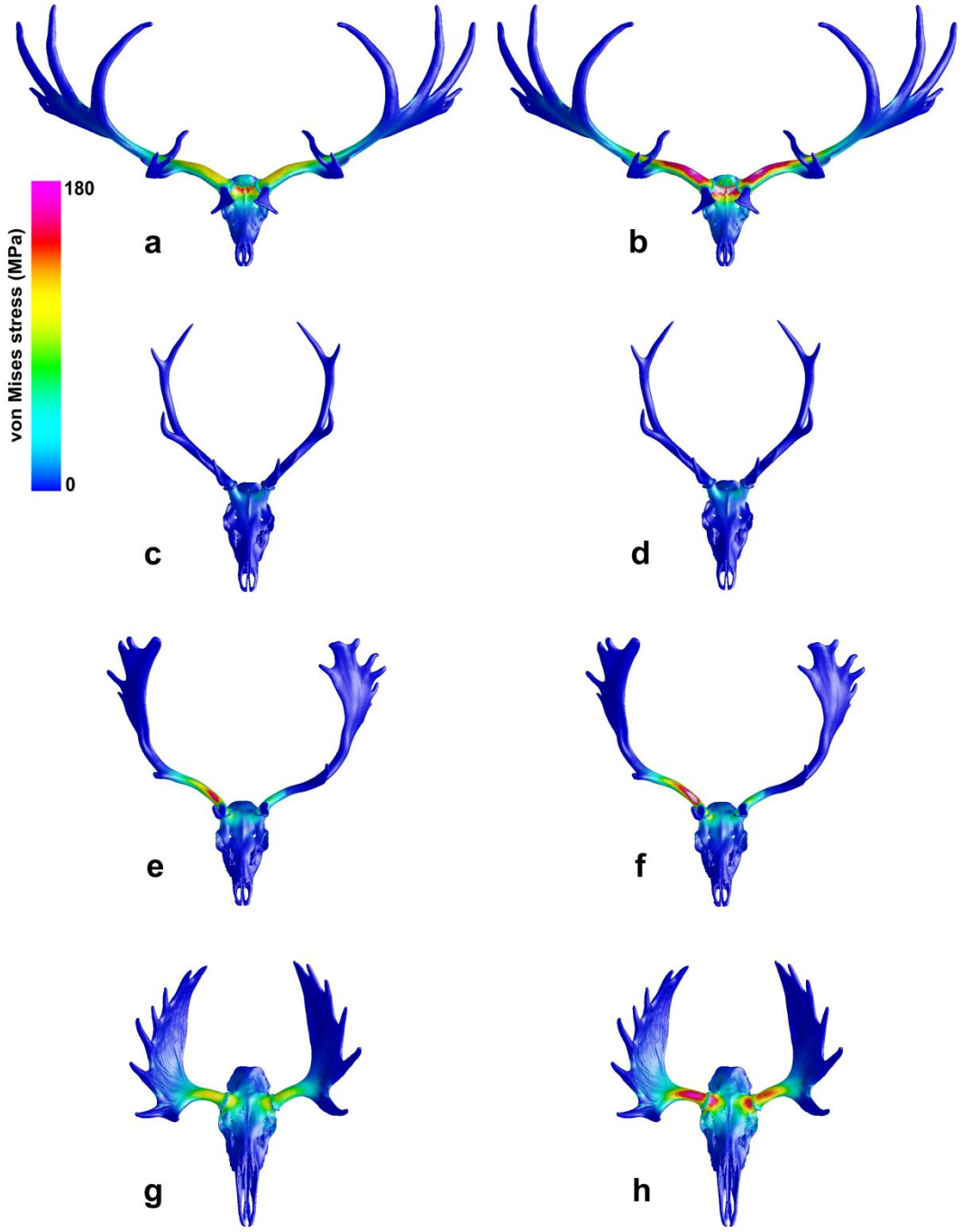

618

619 ~~Figure 5: Unscaled finite element results of a pushing load. a) *Megaloceros giganteus*~~

620 ~~average load case, b) *Megaloceros giganteus* maximum load case, c) *Cervus elaphus* average~~

621 ~~load case, d) *Cervus elaphus* maximum load case, e) Fallow Deer average load case, f)~~

622 ~~Fallow Deer maximum load case, g) Moose average load case, h) Moose maximum load~~

623 ~~case.~~

624

625

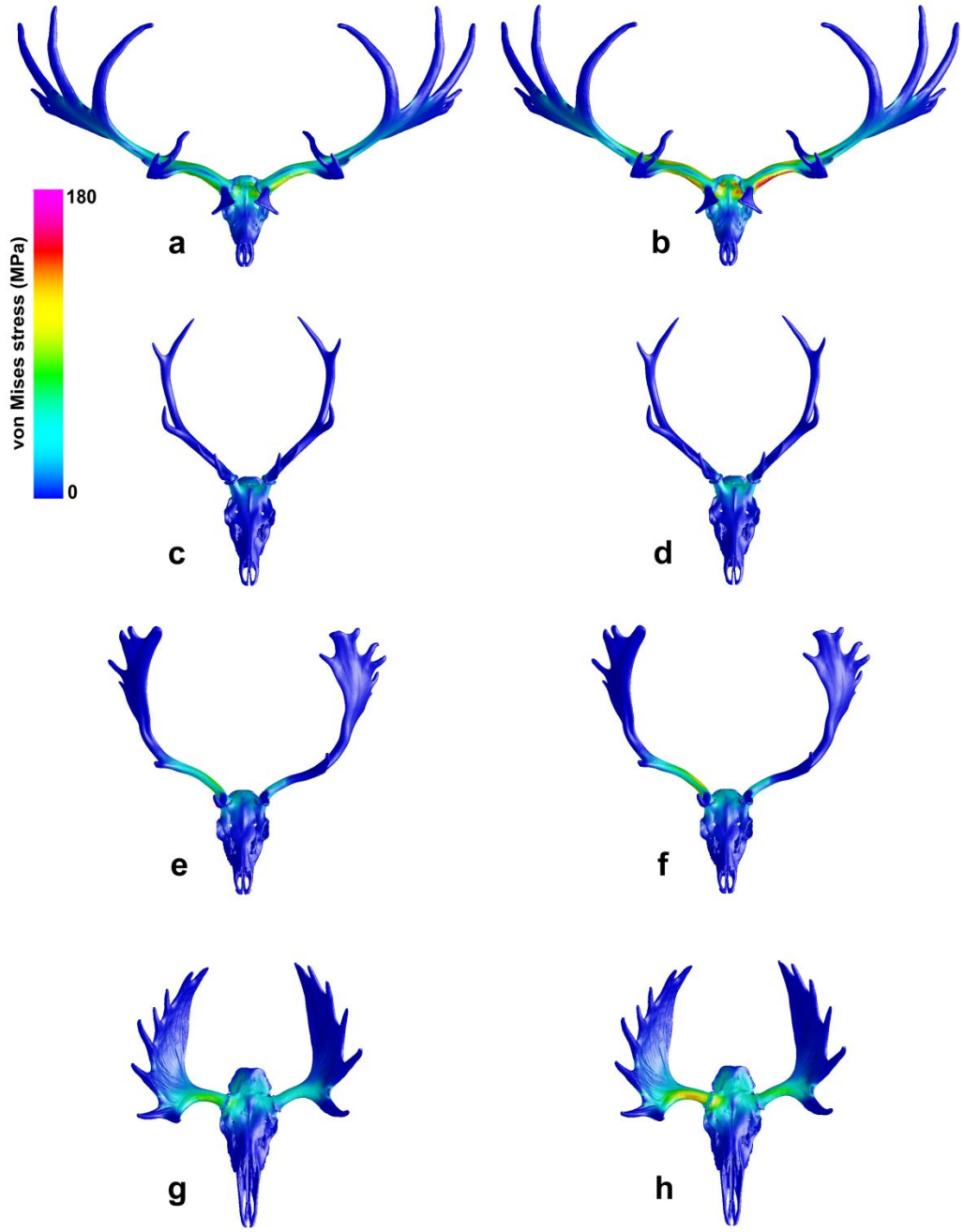

Figure 6: Unscaled finite element results of a twisting load. a) *Megaloceros giganteus* average load case, b) *Megaloceros giganteus* maximum load case, c) *Cervus elaphus* average load case, d) *Cervus elaphus* maximum load case, e) Fallow Deer average load case, f) Fallow Deer maximum load case, g) Moose average load case, h) Moose maximum load case.

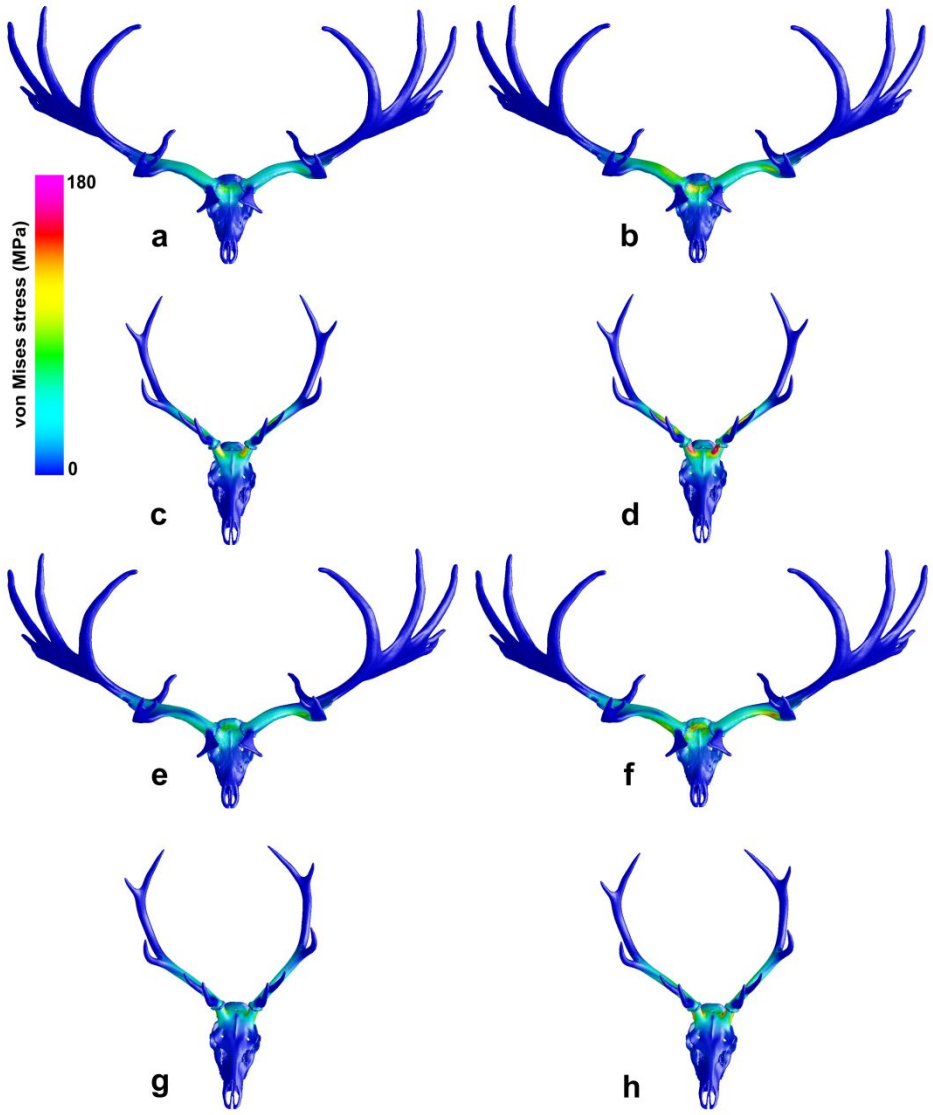

Figure 7: Unscaled finite element analysis results for alternative force placement on *Megaloceros* and *Cervus* under both pushing and twisting loads. Forces in *Megaloceros* were placed more narrowly than in the original analysis, while in *Cervus*, forces were placed more distally on the antlers. Pushing loads: a) *Megaloceros giganteus* average load case, b) *Megaloceros giganteus* maximum load case, c) *Cervus elaphus* average load case, d) *Cervus elaphus* maximum load case. Twisting loads: e) *Megaloceros giganteus* average load case, f) *Megaloceros giganteus* maximum load case, g) *Cervus elaphus* average load case, h) *Cervus elaphus* maximum load case.

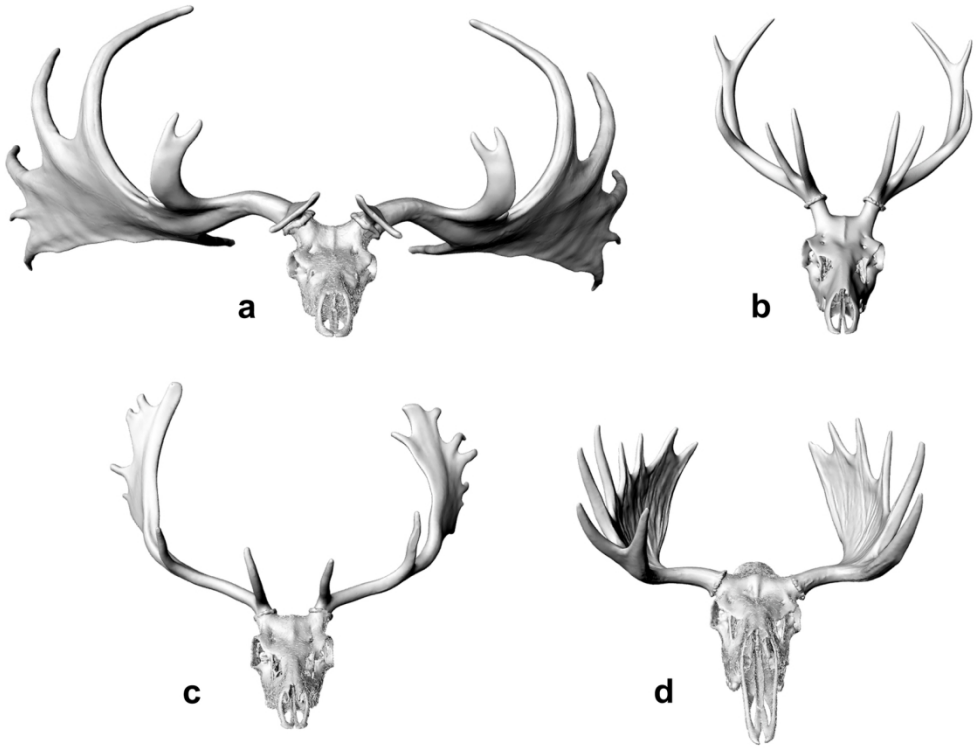

Figure 1: 3D models of the four deer species analysed in this study. a) *Megaloceros giganteus*, b) *Cervus elaphus* (red deer), c) *Dama dama* (fallow deer), d) *Alces alces* (moose). Models have been displayed as approximately the same size for this figure.

154x119mm (300 x 300 DPI)

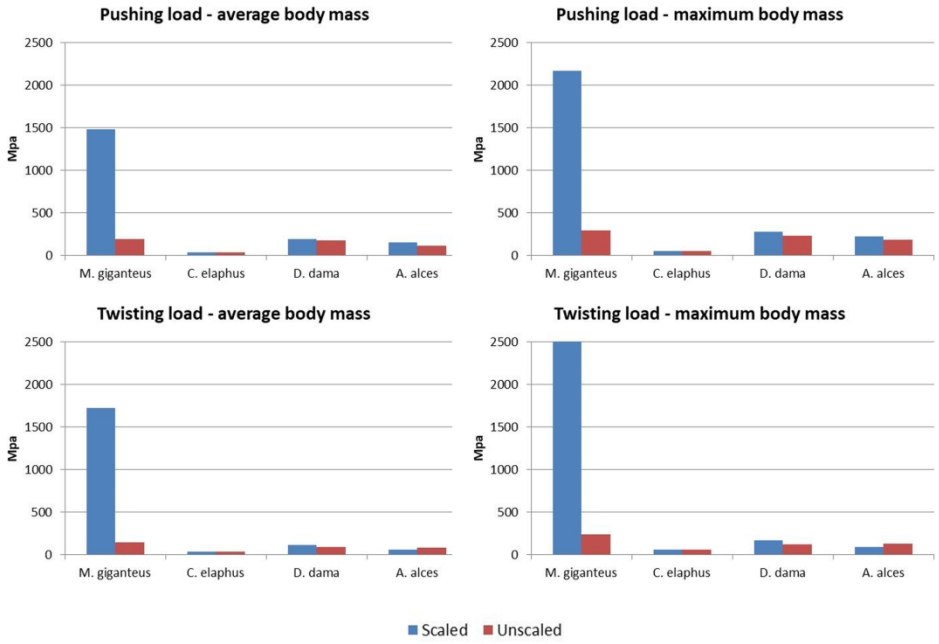

Figure 2: Von Mises stress results in all four taxa under pushing and twisting loads for scaled and unscaled models. Table of results can be found in Supplementary Table 1.

179x123mm (300 x 300 DPI)

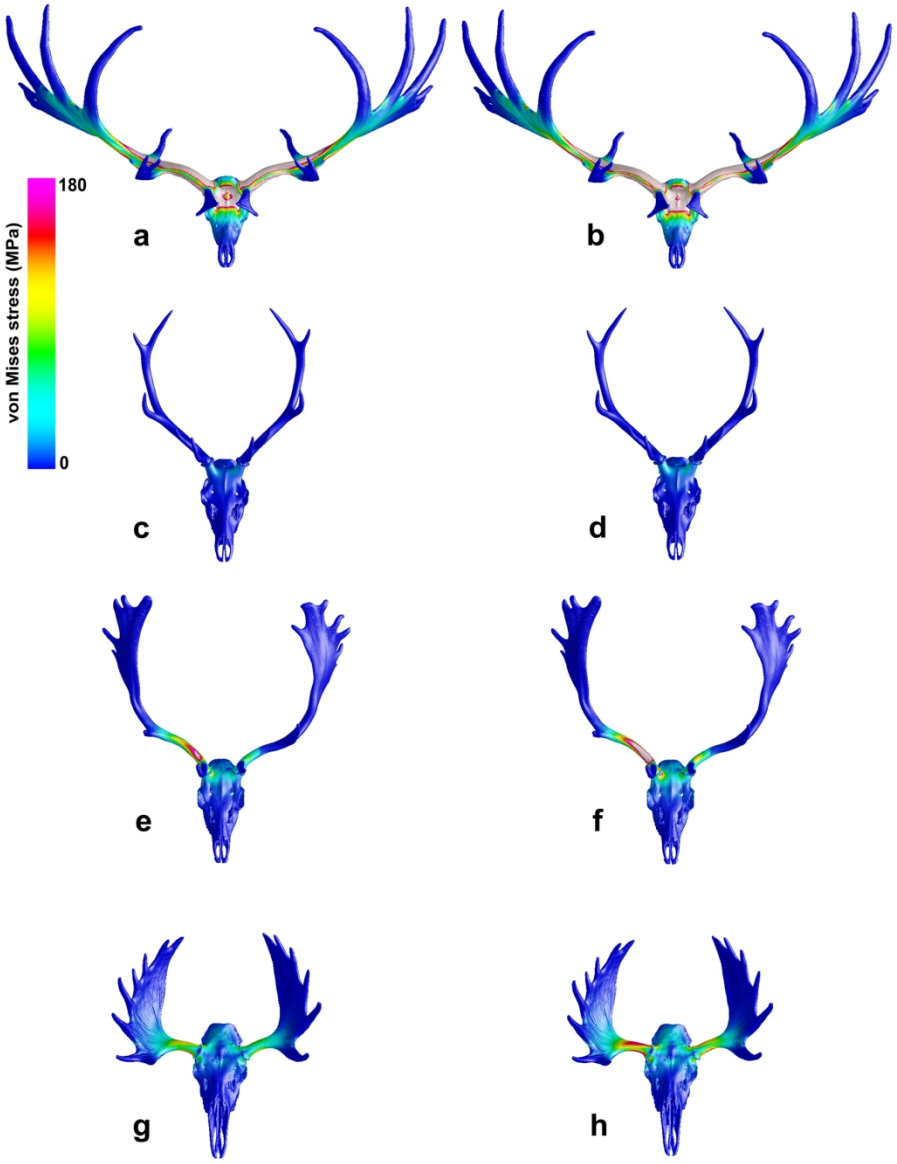

Figure 3: Scaled finite element results of a pushing load. a) *Megaloceros giganteus* average load case, b) *Megaloceros giganteus* maximum load case, c) *Cervus elaphus* average load case, d) *Cervus elaphus* maximum load case, e) *Dama dama* average load case, f) *Dama dama* maximum load case, g) *Alces alces* average load case, h) *Alces alces* maximum load case.

149x197mm (300 x 300 DPI)

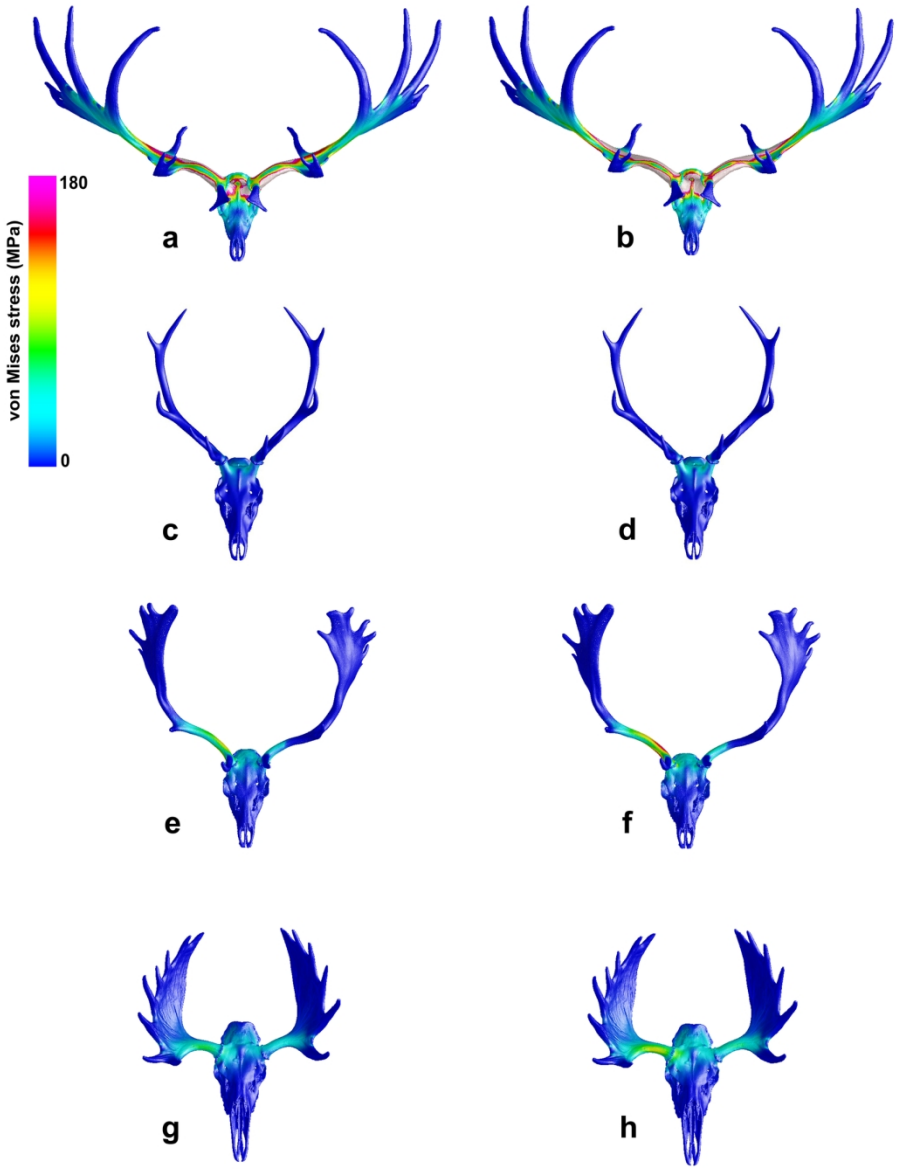

Figure 4: Scaled finite element results of a twisting load. a) *Megaloceros giganteus* average load case, b) *Megaloceros giganteus* maximum load case, c) *Cervus elaphus* average load case, d) *Cervus elaphus* maximum load case, e) *Dama dama* average load case, f) *Dama dama* maximum load case, g) *Alces alces* average load case, h) *Alces alces* maximum load case.

149x193mm (300 x 300 DPI)

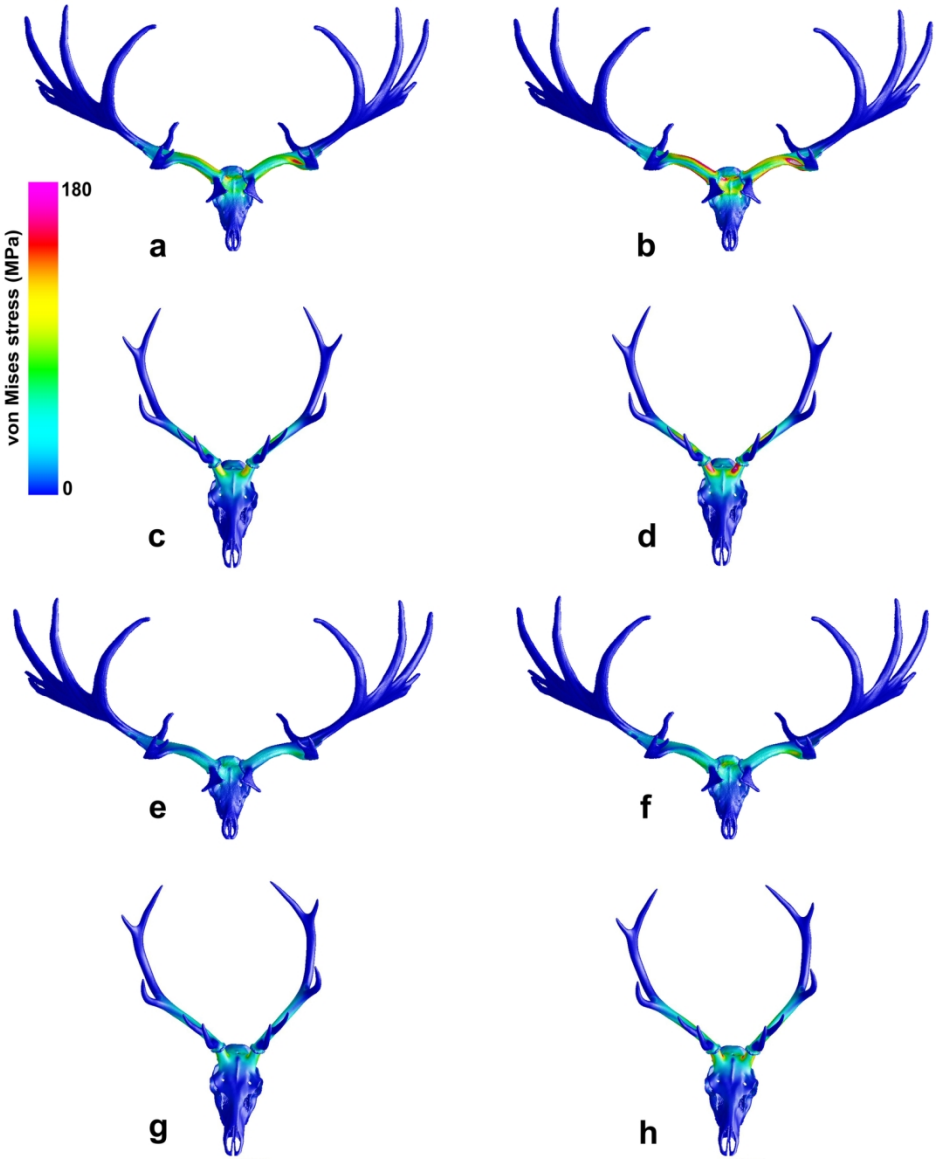

Figure 5: Scaled finite element analysis results for alternative force placement on *Megaloceros* and *Cervus* under both pushing and twisting loads. Forces in *Megaloceros* were placed more narrowly than in the original analysis, while in *Cervus*, forces were placed more distally on the antlers. Pushing loads: a) *Megaloceros giganteus* average load case, b) *Megaloceros giganteus* maximum load case, c) *Cervus elaphus* average load case, d) *Cervus elaphus* maximum load case. Twisting loads: e) *Megaloceros giganteus* average load case, f) *Megaloceros giganteus* maximum load case, g) *Cervus elaphus* average load case, h) *Cervus elaphus* maximum load case.

149x184mm (300 x 300 DPI)